BGSG

Volume 58

Research Paper

THE NORTHERN THESSALY STRONG EARTHQUAKES OF MARCH 3 AND 4, 2021 AND THEIR NEOTECTONIC SETTING

Alexandros Chatzipetros [1], Spyros Pavlides [1], Michael Foumelis [1], Sotirios Sboras [2], Dimitrios Galanakis [2], Christos Pikridas [3], Stylianos Bitharis [3], Evangelos Kremastas [1], Athanassios Chatziioannou [1], Ioannis Papaioannou [4]

[1]**Department of Geology, School of Geology, Aristotle University of Thessaloniki, 54124, Thessaloniki, Greece** ac@geo.auth.gr pavlides@geo.auth.gr mfoumelis@geo.auth.gr ekremast@teemail.com ath.ch.8@gmail.com

[2]**H.S.G.M.E., Hellenic Survey of Geology and Mineral Exploration of Greece, Athens** sboras@noa.gr galanakis@igme.gr

[3]**Department of Geodesy and Surveying, School of Rural and Surveying Engineering, Aristotle University of Thessaloniki, 54124, Thessaloniki, Greece** cpik@topo.auth.gr stylbith@gmail.com

[4]**Civil Engineer- Earthquake Historian, Roidou 10, Larissa, Greece**

Correspondence to:
Alexandros Chatzipetros
ac@geo.auth.gr

DOI number:
http://dx.doi.org/10.12681/bgsg.27225

Keywords:
Earthquake geology, Thessaly, interferometry, modelling, active faults

Citation:
Chatzipetros, A., Pavlides, S., Foumelis, M., Sboras, S., Galanakis, D., Pikridas, Ch., Bitharis, S., Kremastas, E., Chatziioannou, A. and Papaioannou, I. (2021), The Northern Thessaly Strong Earthquakes of March 3 and 4, 2021 and their Neotectonic Setting. Bulletin Geological Society of Greece, 58, 222-255.

Publication History:
Received: 07/06/2021
Accepted: 14/10/2021
Accepted article online: 26/10/2021

The Editor wishes to thank Assoc. Prof. Sotirios Kokkalas and Dr. Christoph Gruetzner for their work with the scientific reviewing of the manuscript and Ms Emmanouela Konstantakopoulou for editorial assistance.

Abstract

A sequence of earthquakes occurred on March 3rd and 4th in Northern Thessaly, northern Greece, associated with previously unknown, blind normal faults within the crystalline Palaeozoic basement of the Pelagonian geotectonic zone. Surficial ground deformation, such as liquefaction phenomena in fluvial plains, as well as soil fissures and rock falls, have been mapped. Geological indications of the unmapped seismic fault, i.e., reactivated shear zones, open cracks, etc., have been identified within the bedrock. Based on geological indications, the main fault projection to the surface could be considered a 15 km NW-SE trending structure and average dip of 45° to the NE. The seismic source of the main shock was modelled, and the Coulomb static stress changes calculated for receiver faults similar to the source. The determination of the active tectonic regime of the region by geodetic data and the well-known faults of NE Thessaly plain are also presented, as well as the revised historical and instrumental seismicity. This earthquake raises new concerns and challenges, revising some established views, such as the status of main stress orientations, the orientation of active tectonic structures, the occurrence of a seismogenic fault in a mountainous massif of crystalline rocks without typical geomorphological expression and the role of blind faults in Seismic Hazard Assessment.

Keywords: *earthquake geology, Thessaly, interferometry, modelling, active faults*

Περίληψη

Μια σειρά σεισμών σημειώθηκε στις 3 και 4 Μαρτίου 2021 στη Βόρεια Θεσσαλία, (Βόρεια Ελλάδα), που σχετίζεται με προηγουμένως άγνωστα, τυφλά κανονικά ρήγματα στο κρυσταλλικό παλαιοζωικό υπόβαθρο της Πελαγονικής γεωτεκτονικής ζώνης. Έχουν χαρτογραφηθεί επιφανειακές παραμορφώσεις του εδάφους, όπως φαινόμενα ρευστοποίησης σε πεδιάδες του ποταμού, καθώς και ρωγμές εδάφους και καταπτώσεις βράχων. Εντοπίστηκαν γεωλογικές ενδείξεις για το μη χαρτογραφημένο σεισμικό ρήγμα, δηλαδή ζώνες διάτμησης που επανενεργοποιήθηκαν, ανοιχτές ρωγμές κ.λπ. Με βάση τις γεωλογικές ενδείξεις, η κύρια προβολή ρηγμάτων στην επιφάνεια θα μπορούσε να θεωρηθεί ως μια δομή 15 χλμ ΒΔ -ΝΑ διεύθυνσης και μέσης κλίσης 45^{o} στα ΒΑ. Η σεισμική πηγή του κύριου σεισμού μοντελοποιήθηκε και οι αλλαγές στατικής τάσης Coulomb υπολογίστηκαν για ρήγματα παρόμοια με την κύρια σεισμική πηγή. Παρουσιάζεται επίσης ο προσδιορισμός του ενεργού τεκτονικού πεδίου της περιοχής με γεωδαιτικά δεδομένα και τα γνωστά ρήγματα της ΒΑ Θεσσαλικής πεδιάδας, καθώς και η αναθεωρημένη ιστορική και ενόργανη σεισμικότητα. Αυτός ο σεισμός εγείρει νέους προβληματισμούς και προκλήσεις, αναθεωρώντας ορισμένες απόψεις, όπως η κατάσταση των κύριων προσανατολισμών τάσης, ο προσανατολισμός των ενεργών τεκτονικών δομών, η εμφάνιση σεισμογόνου ρήγματος σε ορεινό όγκο κρυσταλλικών πετρωμάτων χωρίς τυπική γεωμορφολογική έκφραση και ο ρόλος των τυφλών ρηγμάτων στην εκτίμηση σεισμικού κινδύνου.

Λέξεις - Κλειδιά: *γεωλογία των σεισμών, Θεσσαλία, συμβολομετρία, προσομοιώσεις ενεργά ρήγματα*

1. INTRODUCTION

The region of Thessaly lies at the central part of Greece and is characterized by an active tectonic regime, as well as by occasional destructive seismic events. The most recent geological structures of the area derive from two phases, i) the Pliocene – Lower Pleistocene phase with NW-SE-trending grabens and horsts, formed by the post-orogenic collapse which is associated with the NE–SW extensional (σ_3) pattern of the area, and ii) the Middle Pleistocene – Holocene phase with E-W- to ESE-WNW-striking normal faults, related to the N–S to NNE–SSW oriented extensional regime.

The strong earthquakes of March 3rd and 4th 2021 (Mw 6.3. and 6.0 respectively) and their aftershock sequence affected a large area of northern Thessaly. The seismogenic volume, that is the aftershock sequence, extends from the Antichasia mountain basement, up to Titarissios river valley (Fig. 1). Along the same valley, liquefaction phenomena as well as a NW-SE trending line of open fractures were observed and mapped. As suggested by all preliminary published focal mechanisms, an unknown-unmapped inherited tectonic structure represented by two low to moderate dipping fault planes was responsible for both strongest shocks respectively (Fig. 2). The Pelagonian basement which hosts this structure is a complex alpine edifice according to Kilias et al. (2013, 2016) having undergone many intense compressional phases with folding and thrusting, as well as an ultimate alpine extensional phase imprinted by low and moderate dipping normal faults.

We conducted a multidisciplinary study of the North Thessaly seismic sequence in order to define the seismic fault(s) and its (their) attributes, to track and interpret the complex primary and secondary ground deformation phenomena, to estimate the effect of the mainshock on nearby tectonic structures, and to explain the change of the active stress field orientation.

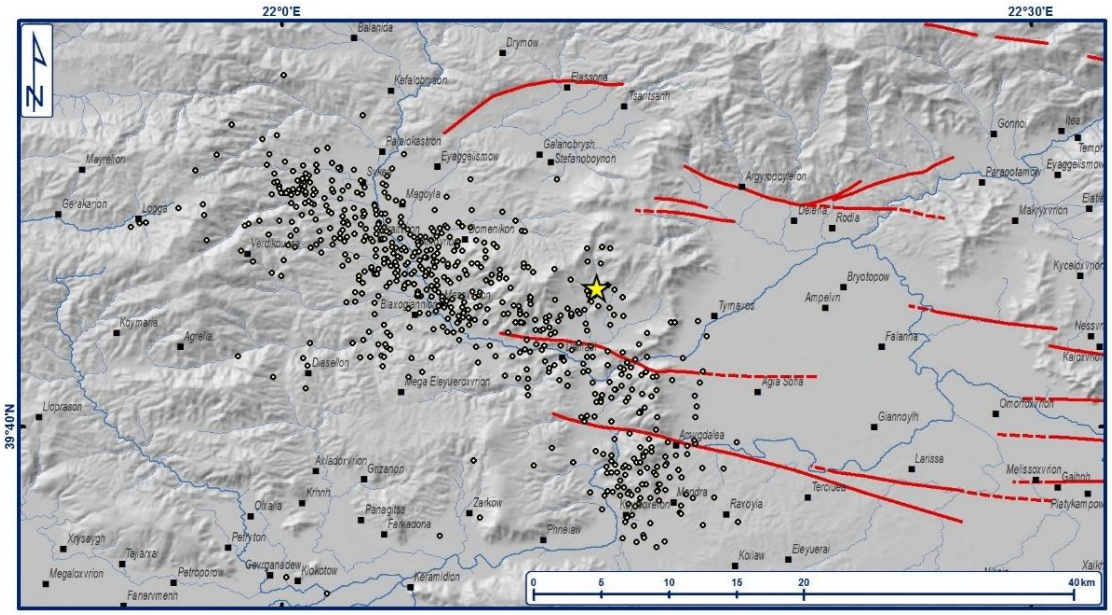

Fig. 1: The mainshock (yellow star) and the aftershock sequence (circles), aligned in a NW-SE direction. Red lines show the known active faults of the affected area (solid lines: mapped faults, dashed lines: inferred location).

Concerning the seismic history of the broader study area, during the 20th century, an earthquake of similar magnitude (M_S 6.3) occurred in Larissa on March 1, 1941, exactly 80 years ago, with severe damages and casualties for the city and the surrounding

villages, mainly in the eastern Thessalian plain. This event is associated to the Asmaki fault, Fig (Caputo et al., 2004, Papaioannou, 2018).

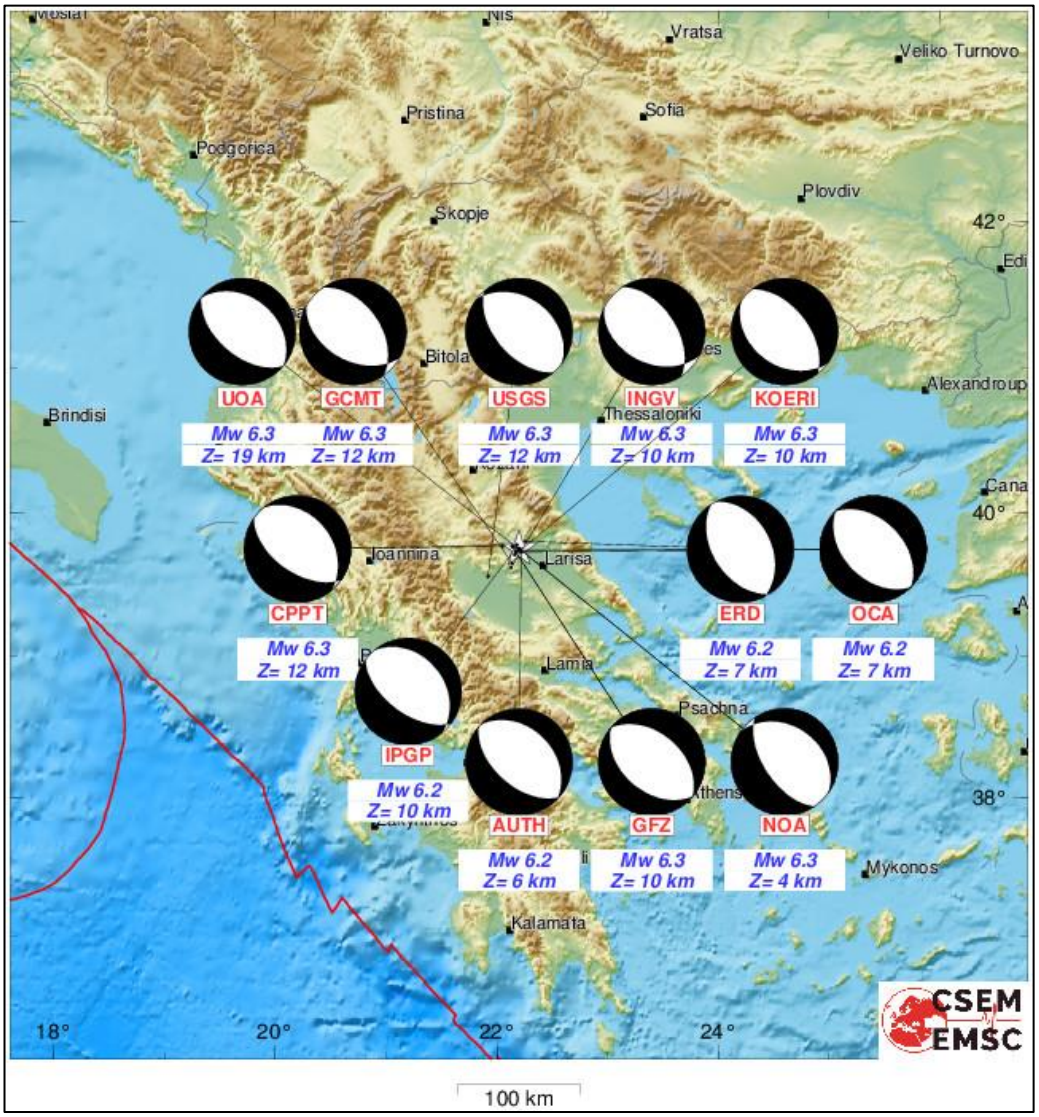

Fig. 2: Quick MT solutions, as published by various institutes (source: EMSC).

An earlier earthquake of M5.6 occurred in the northwestern area in November 1901. The epicentre of the strong historical earthquake in 1735 is possibly located in the same area and may be associated to this fault or other similar local structures. Other active geological structures of the region lie within the Larissa plain and include the Gyrtoni (GF), Rodia (RF), Elassona, Gonoi, Tempi and Omolio (OF) faults (Fig and GreDaSS http://gredass.unife.it), which are currently being studied using advanced methods (satellite imagery analysis, high resolution UAV models, geodetic, geological and paleoseimological ones; e.g. Tsodoulos et al., 2016; Kremastas et al., 2018; Lazos et al., 2021). It is worth mentioning at this point that the first author who referred to earthquakes as a possible cause of formation of Tempi valley, with the contribution of God Poseidon, was the historian Herodotus (485-425 BC).

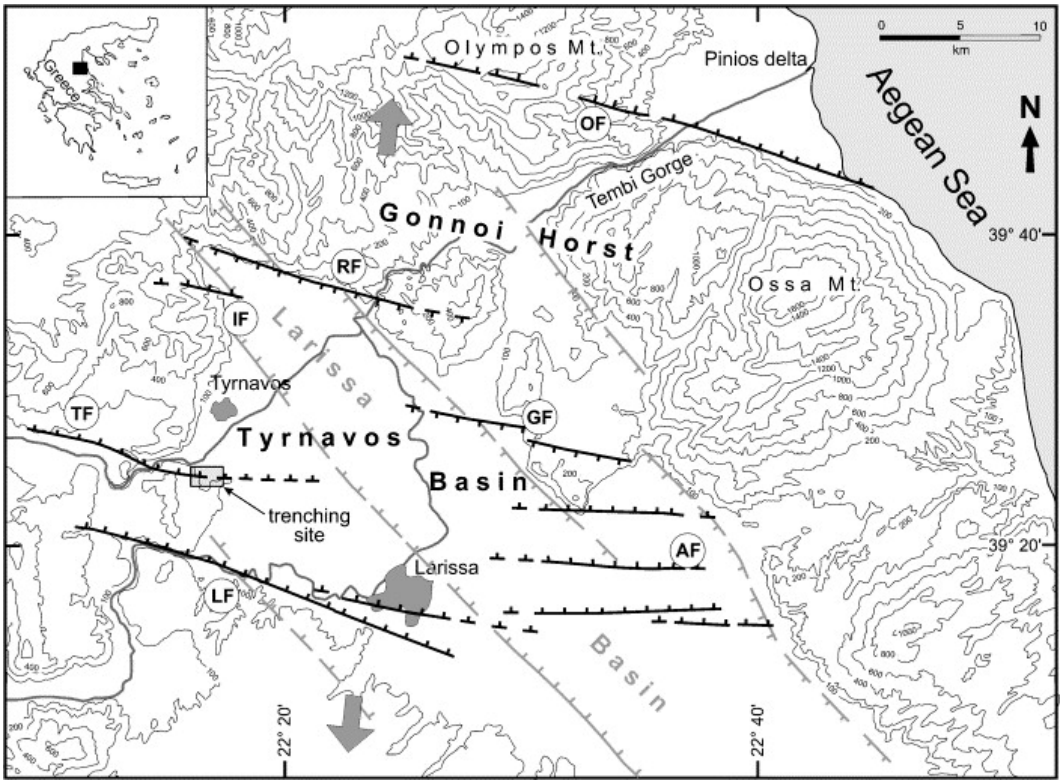

Fig. 3: Simplified tectonic map of the study area, after Caputo et al. (2004). TF: Tyrnavos fault, LF: Larissa fault, GF: Gyrtoni fault, RF: Rodia fault, AF: Asmaki fault, OF: Omolio fault.

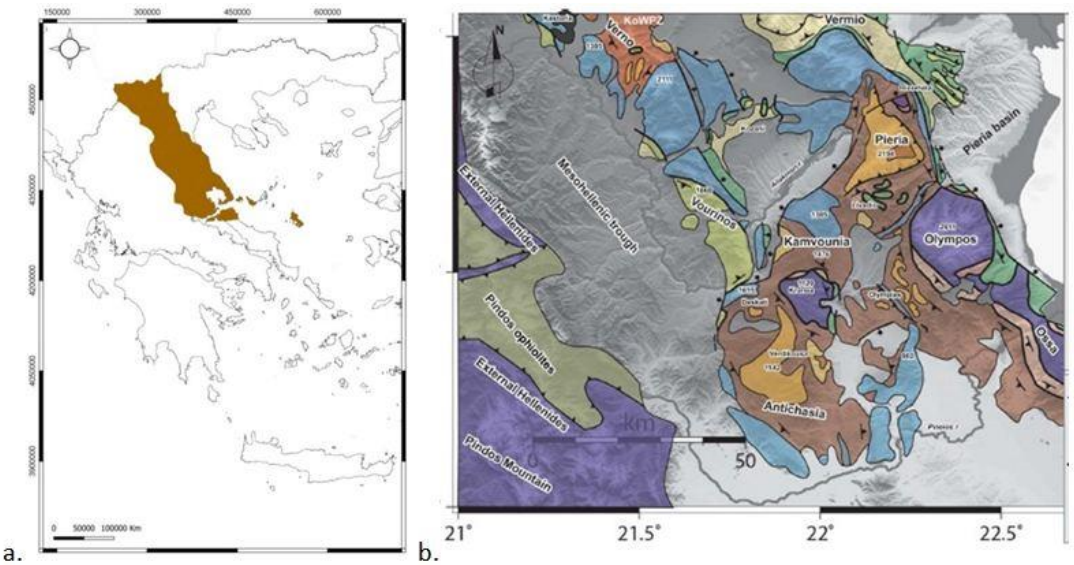

Fig. 4: a) The extend of the Pelagonian geotectonic zone in the Hellenic orogenic system. B) Geological map of part of the Pelagonian rocks in Thessaly and western Macedonia. The tectonic windows of Olympos, Krania and Rizomata are indicative of the post-orogenic collapse through low-angle normal detachment faults (Kilias and Mountrakis, 1989; Koroneos et al., 2013).

2. GEOLOGICAL SETTING

2.1. Alpine Geology-Tectonic Evolution

The study area belongs to Pelagonian geotectonic zone of Greece (Fig. 4a) and it is composed of crystalline metamorphosed Paleozoic and possibly pre-Paleozoic rocks (Fig. 4b). The accumulation of successive nappes in conjunction with the development of subducted zones, is associated with two HP/LT metamorphic stages. The extensional regime that followed the nappe tectonics led to the collapse of the orogen through large normal low angle detachment faults, and the exhumation of underlying units as tectonic windows (Lister et al., 1984; Kilias et al., 1991, 2002, 2016; Sfeikos et al., 1991; Dinter and Royden, 1993; Kilias, 1995; Forster and Lister, 1999). The extensional tectonics has played an important role from the Tertiary until today with extensive shear zones and detachment faults (Fig.). The reactivation of the inherited structures as inverse tectonics is a question under review in relation to the 2021 earthquake sequence.

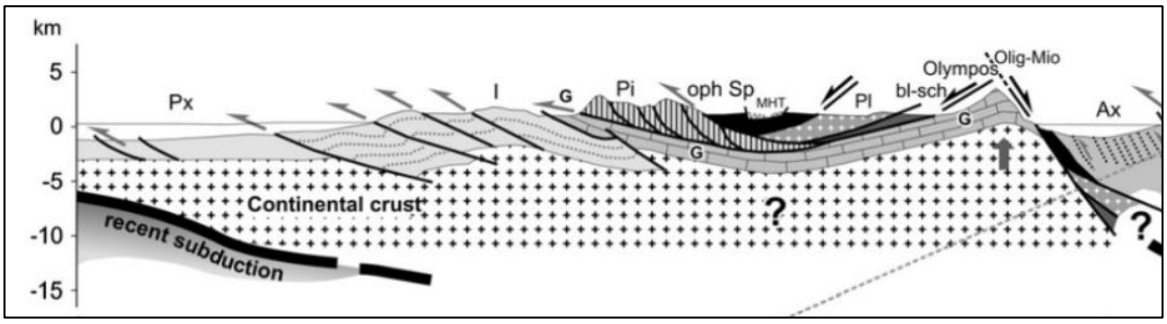

Fig. 5: Interpretation of the current geotectonic model of the broader area. SW-NE cross section, modified from Kilias et al. (2013a).

The study area has a more complex picture of tectonic deformation, as several tectonic events have affected its rocks according to Kilias et al. (1991, 2013), who give a complete picture of the deformation sequence. A dominant S1 schistosity is recognized in the wider area. It is oriented to the SW south of the tectonic window of Krania and to the NE to the north. Lineament L1 is recognized on the S1 planes, with a constant direction NE-SW to NNE-SSW. S1 and L1 are due to a deformation event (D1) associated with the overthrusting of the Pelagonian basement on the carbonate series from NE to the SW. In the last stages of D1 deformation, extensional SB shear zones are created, as well as low angle normal faults in the uppermost tectonic horizons, dipping to the SW and NE. This is followed by a second D2 compressive deformation

event with very low P/T conditions, characterized by knick folds, shear zones and thrust faults.

2.2. Neotectonic regime and seismogenic sources

Since Middle Miocene, the study area is being deformed under an extensional stress field. The first post-orogenic collapse phase has a NE-SW direction of extension. This phase started in Late Miocene and lasted until Pliocene in the area. This extensional configuration has migrated to the west, following the outward migration of the orogenic front due to the roll-back of the subducting plate. It is still active in Epirus and Albania (Pavlides and Kilias, 1987; Mercier et al., 1989; Caputo and Pavlides, 1993; Mountrakis, 2006). This phase is the one that has formed the large, NW-SE trending basins of western Macedonia and Thessaly.

The active extensional field has been active since Middle Pleistocene, has a N-S general trend and affects the broader Aegean area. It caused the formation of a new generation of E-W trending normal faults, which are currently defining the northern boundary of Thessaly plain (Fig. 6).

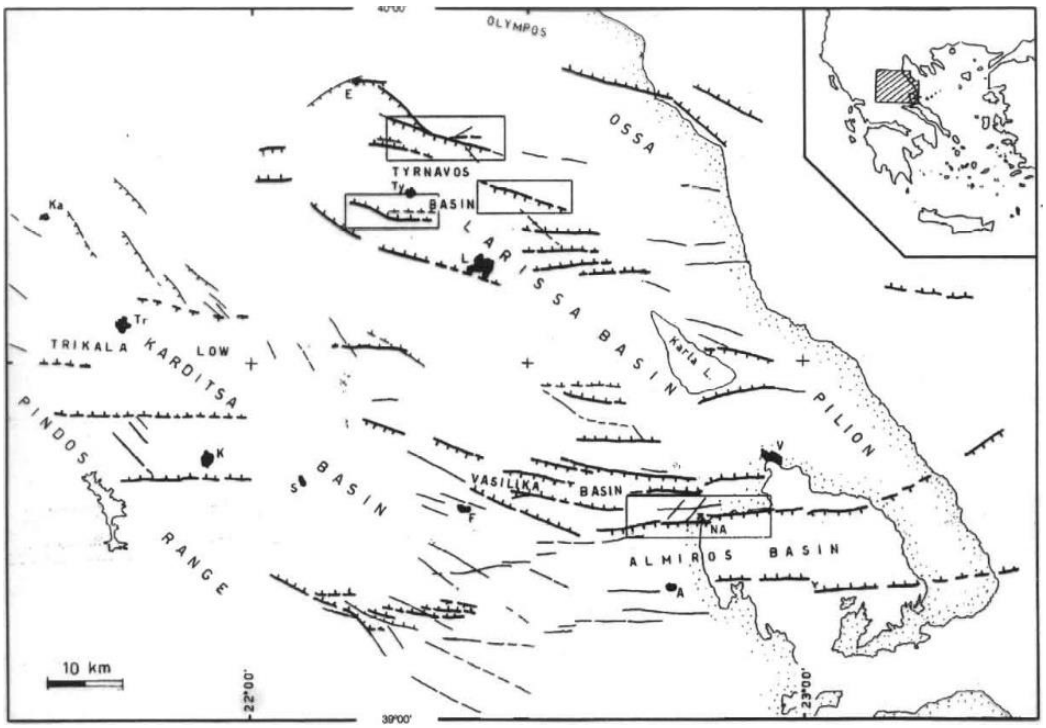

Fig. 6: Simplified tectonic map of Thessaly (Caputo and Pavlides, 1993; Caputo, 1995). The main Quaternary faults are shown in thick black lines, the teeth indicating the hangingwall.

The Tyrnavos fault is a typical tectonic structure considered as active, similar to many others in the broader area (Caputo and Pavlides, 1993; Caputo, 1995; Caputo et al., 2004). It strikes WNW-ESE and has a surficial length of 10-12 km. This fault is one of the best studied active structures in Greece for more than 30 years by the Earthquake Geology research team (AUTh) and the University of Ferrara (Italy) and is included in the Greek Database of Seismogenic Sources (GreDaSS http://gredass.unife.it, Fig. 7; Sboras, 2011; Caputo et al., 2012, 2013, 2014; Caputo and Pavlides, 2013; Sboras et al., 2014), in which it is described in detail. According to geological data, geophysical surveys and palaeoseismological excavations which study the geological history of the fault, document slow activity characterized by vertical surficial co-seismic displacements of 20-40 cm and a possible recurrence period of about 1-2.5 ka, as well as a low slip rate of 0.05-0.25 mm/year. Its earthquake potential is estimated to M 6.1 to 6.3 (Caputo et al., 2004), based on the empirical relationships Ms *versus* SRL of Pavlides and Caputo (2004) and Wells and Coppersmith (1994). The active deformation of the area is also well documented by recent satellite geodetic analysis (Chatzipetros et al., 2018; Lazos et al., 2021).

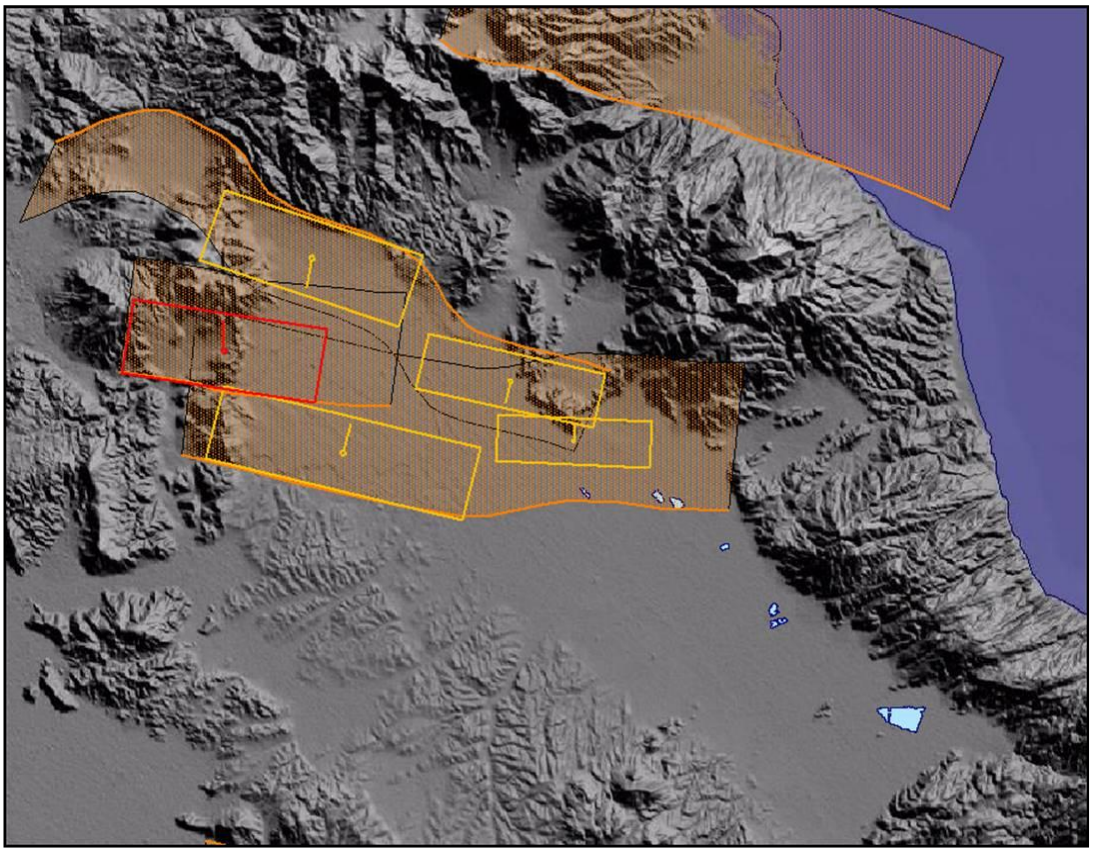

Fig. 7: The northern Thessaly fault system, as shown in the Greek Database of Seismogenic Sources (GreDaSS). Boxes are rough approximation of the vertical projection of the fault plane to the surface.

3. THE ELASSONA NEOGENE-QUATERNARY BASIN

The Elassona Basin comprises the southernmost part of the Florina-Ptolemaida-Kozani-Sarantaporo-Elassona Neogene tectonic depression, and it is known for the hosted coal deposits. The basin can be further divided into two sub-basins, the north-eastern one, where the town of Elassona lies, and the southwestern one (Potamia sub-basin), where the Domeniko, Amouri, Evangelismos and Mesochori villages are located. The latter sub-basin is located within the meisoseismal area of the March 2021 earthquake sequence. The two sub-basins are connected through the Aghioneri narrows and the Elassonitis River valley, while the Potamia sub-basin becomes narrower to the east before entering the Titarissios River valley.

The combination of neotectonic, palaeoclimatic and palaeogeographic conditions facilitated the basin formation and its filling with new sediments. Thus, the inner part of the basin is filled with Neogene and Quaternary deposits in which the lignitic deposit occurs. The Pliocene formation unconformably overlie the alpidic crystalline basement due to the intense alpidic tectonic activity that took place before the Neogene sediments deposition.

During the exploration campaign in the area by the Institute of Geology and Mineral Explration of Greece (Dimitriou & Giakoupis, 1998), a dense network of boreholes was drilled revealing important tectono-stratigraphic information for the Potamia sub-basin (see also Galanakis et al., 2021; this volume). According to this study, besides the topmost Holocene deposits, the underlying Upper Miocene to Pliocene formations are often observed vertically displaced from borehole to borehole, implying the occurrence of normal faulting. All implied faults are not of the same age since they either displace the deeper Upper Miocene formations, or the displace the base of Quaternary (Villafranchian). The younger faults, characterized as “post-Neogene” faults in the study, demonstrate a NW-SE direction forming bookshelf or graben-style patterns. Besides this study, along the SW margin of Potamia sub-basin, a fault of similar direction (dipping to the NE) is mapped, having created a downthrow of several tens of metres. This fault lies on the extension of the co-seismic ground ruptures and the liquefaction phenomena which were mapped south of the Titarissios river. Possible co-seismic ruptures or gravitational ones appeared after the earthquake on a NNW-SSE trending fault between the villages Amouri and Vlachogianni. This place is key to understanding the neotectonics of the wider area and especially the active tectonics.

4. HISTORICAL SEISMICITY

Concerning the historical seismicity of the region, important details and revisions are included in (Papaioannou, 2017a, 2017b, 2018, 2019). The epicentre distribution of the main earthquakes is given in Fig. 8. On 12/25 November 1901 according to old and new calendar respectively, at approximately 5 a.m. local time, a strong earthquake caused damage to the houses of the village Verdikoussa again, where 4-5 houses collapsed. It provoked a large landslide, as well. The information comes from a report by the Greek Consulate in Elassona (the area of Elassona was, then, under Ottoman rule), to the Greek Ministry of Foreign Affairs. Based on this macro-seismic information, it is estimated that the epicentre was reported close to Verdikoussa (geographic coordinates 39.80 ° N; 22.10 ° E) and its magnitude estimated M 5.6 +- 0.2 (possibly 5.8).

In previous seismic historical research have been referred two strong earthquakes in northern Thessaly, that of 1735 (Papazachos and Papazachou, 2003; Ambraseys, 2009) and the unknown 1901, which, most likely, occurred in the same seismogenic area of the recent earthquakes of Larissa – Tyrnavos -Elassona and in fact in northeastern part (area of Verdikoussa-Pretori villages, Fig 8 or coordinates 39.80° N; 22.00° E). The first occurred on 21 August (old calendar) / 1 September (new calendar) 1735. It was an earthquake that lasted a long time and shook Larissa city. This emerges from the following memoir written in ecclesiastical book, as follows: “On that year 1735 in the month of August 21st a great earthquake occurred”. “The quake itself caused cracks in the church of Holy Monastery of Barlaam of Meteora, as well as in the dining room and in the kitchen. Earthquakes followed that lasted 15 days (aftershocks)”.

From the above descriptions, it has been estimated that the earthquake probably was created from the same seismogenic area of the recent earthquakes (March 2021), which is located between Larissa and Kalambaka and strongly felt but were also slightly harmful in both cities. Intensity of the EMS-98 scale is estimated at VI in Larissa and V-VI in Kalambaka, where fallen rocks observed from the characteristic rocky monasteries of Meteora. Based on the distribution of macro-seismic information, it is estimated that the epicenter of the earthquake was located between Verdikoussa and Pretori (geographical coordinates 39.80° N; 22.00° E) and that its approximate magnitude was M 6.2, with a standard deviation of 0.2. This estimated position of the epicenter is located 18 km NW of the epicenter of the earthquake of March 3, 2021 and is 33 km away from the Varlaam Monastery of Meteora and 40 km from Larissa.

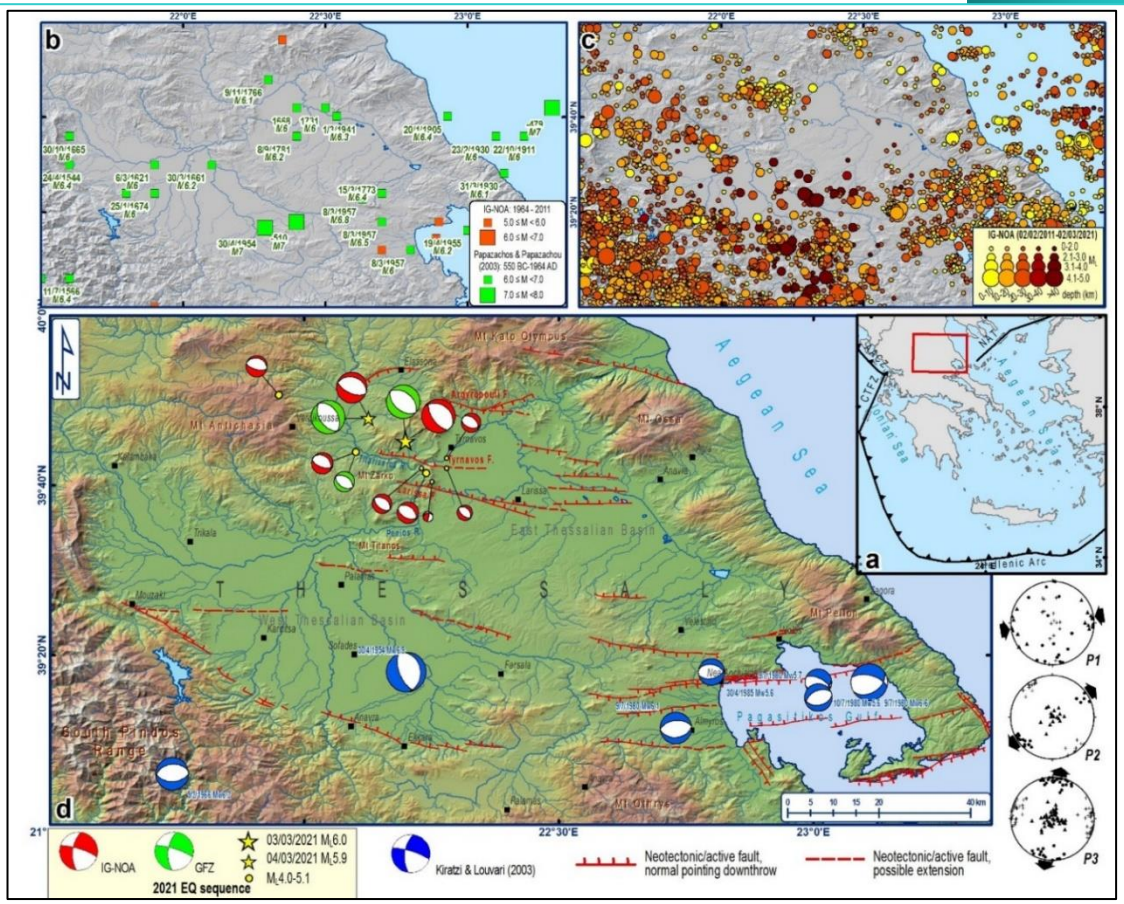

Fig. 8: Historical seismicity in the study area. The lower map shows the focal mechanisms of the main instrumentally recorded events in the area, as well as the ones of the March 2021 sequence.

Concerning the 1766 strong earthquake, which is referred in bibliography as an earthquake of the area (M 6.3; I_{max}=VIII, Elassona, 39.7º N; 22.2º E), we think that this is not a correct attribution. On October 28 / November 8, 1766, this strong event caused significant damage to homes and chimneys in an unnamed area, which in the current literature is considered to be Elassona town. Furthermore, the earthquake was strongly felt in Zakynthos (Zante, Ionian Sea), it had long duration and caused great concern to the inhabitants, who woke up, got out of their houses and took refuge in churches, praying. The information about this earthquake came from two sources: a) From a memoir written in a musical manuscript of Olympiotissa Monastery (Elassona), which states the following: "During 1766 October 29 in the evening of Sunday, around 4 o'clock at night, a great earthquake happened, so that many houses were shaken and damaged". The author of the manuscript, Constantine, was the lead cantor of the church of Ioannina (Epirus). The manuscript was written in 1717, forty-nine years before earthquake, as referred to the following note, in same manuscript: "*the present was coming to an end "Asmatomelirritofthongos" book in the year of salvation, Psafiz 'ω [= 1717]: εν μηνί ιουνίω θ'η: μέρα σαββάτω. It was written by me poor, minimal and*

ignorant Constantine, and protopsalt (lead cantor) of the great church of Christ, and famous city of the metropolis of Ioannina". Fifty years later, in January 1767, Anthimos Olympiotis became the owner of the manuscript, as is mentioned in another chronological note of the same manuscript: "*This is property of Anthimos Hieromonk of his meadow (sic) 1767 January….* " At that time Anthimos was serving as pastor and teacher in Miskolc, Hungary. Between 1717 and 1767, there is no other reference of ownership of the manuscript. It is very likely that the manuscript was purchased at Ioannina, on behalf of Anthimos, by his friend Georgios Patakis from Epirus, soul of the Greek community in Miskolc. It is well known that Anthimos, after his studies, served from the spring of 1762, as pastor and teacher in the cities of Ketskemet in Hungary and Miskolz and then as a pastor in the Austrian capital city, Vienna. In October 1777, he returned to the Olympiotissa monastery (Elassona). Upon his return he donated, besides among others, his personal library which contained 400 volumes of books, 10 of which he had compiled during fifteen years abroad. Among the books was the aforementioned manuscript, which was acquired ten years ago while in Miskolc. Therefore, the memoir was not written by Anthimos Olympiotis in Elassona, since in November 1766 he was in Hungary and had not yet become the owner of the manuscript. b) From a memory of the notary of Zakynthos Stathis Papadatos, who recorded it in a notebook stating the following: "*1776 October 28. Monday dawn 11 at 5 of the night a big earthquake happened starting slowly at first and gradually becoming stronger. The people got up and asked for forgiveness, they ran to churches*".

From the examination of the macro-seismic results described in the two memoirs, it is unlikely that the earthquake could have its epicentre in Elassona area. There was, a few years ago in Ioannina, an earthquake with epicentre in the broader area of Ioannina. This event could have caused in the city of Ioannina, the damages described by first memoir and could be strongly felt in Zakynthos, as described in the second one. In the broader area, earthquakes of magnitude 6.0 to 6.3 are rather common and have caused damages repeatedly in Ioannina city. From a similar earthquake of magnitude 6.3, which occurred on July 31, 1898, in this area, buildings and chimneys collapsed in Ioannina, while it was strongly felt in Zakynthos. Following all the above arguments, the earthquake of October 28 / November 8, 1766, must have occurred in the area of Ioannina (Epirus) and not in the area of Elassona, as previously thought. This is a revision of the catalogue of known historical earthquakes in the region. Another large earthquake in the broader area occurred on 1892 (Papazachos and Papazachou, 2003; Ambraseys, 2009; Papaioannou, 2017a, 2019), while there is information about an earthquake of 1781 of a similar magnitude.

5. GPS GEODESY AND THE TECTONICS OF THE REGION

Concerning the crustal deformation of Thessaly due to active tectonics, raw data for a seven-year period were collected from 27 permanently installed GPS/GNSS stations, and processed using by the triangulation methodology (Lazos et al., 2021). From this methodology a series of parameters was calculated including maximum horizontal extension, total velocity, maximum shear strain, area strain and rotation (Fig. 9). The maximum horizontal extension parameter shows a dominant N–S direction, which is consistent with the active fault zones of the broader Thessaly area. However, sparse distribution of E–W maximum horizontal extension vectors is documented, while it is likely to be associated with local tectonic structures; limited compressional occurrences are also observed at the western part of the study area. Regarding the total velocity, the estimated vectors are characterized by a NE–SW direction, leading to the conclusion that the broader Thessaly area show a SW motion, receiving the highest and lowest values at its southern and northern parts, respectively. Maximum shear strain is directly related to the activation of fault zones, while the highest values are observed at the eastern part of Thessaly, close to the North Aegean region.

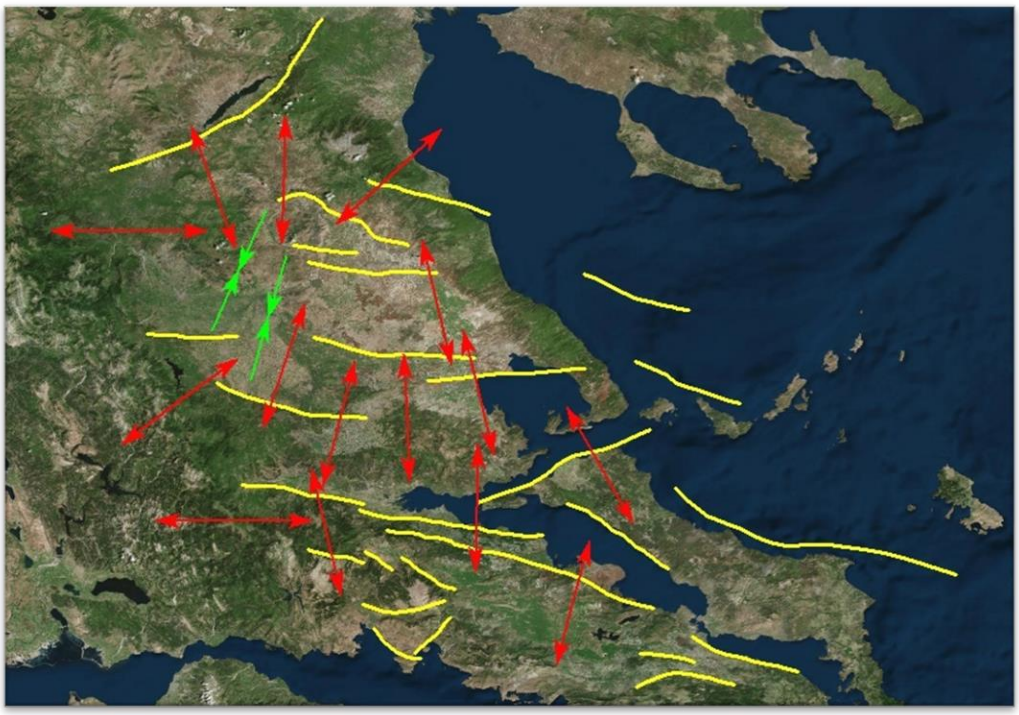

Fig. 9: Representative maximum horizontal extension (red) and contraction (green) vectors of the study.

The recent activity of the North Aegean fault zones (seismic events) was imprinted at the raw geodetic data, leading to high maximum shear strain values. Regarding the area strain parameter, it is associated with the dilatation and contraction of the study area.

The highest contraction values are documented at the western part of the study area, close to the Pindos Mountain range, where compressional tectonics occur, while the highest dilatation values are recorded at the Pagasitikos Gulf region, coexisting with high contraction values. This coexistence of dilatation and contraction indicates potential strike-slip structures, leading to the conclusion that the wider Pagasitikos Gulf area is probably affected by the North Aegean Trough fault zones activity, constituting the westward continuation of the North Anatolian fault zone. The rotation parameter shows a dominant clockwise rotation of the area, while limited and local-scale counter-clockwise rotation vectors are also documented.

6. THE MARCH 3 AND 4, 2021, EARTHQUAKES – ENVIRONMENTAL EFFECTS

The earthquake sequence produced secondary surface effects, as the seismogenic fault did not reach the surface. The surface effects were distributed throughout the affected area (Fig. 10) and have been briefly presented in preliminary publications (Ganas et al., 2021; Pavlides et al., 2021; Valkaniotis et al., 2021). The majority of the surface ruptures were observed in Titarisios river valley (Fig. 11), while the bulk of liquefaction occurred in Pinios river valley. The main features are described in the following paragraphs, based on original fieldwork and observations.

6.1. Liquefaction phenomena

Dozens of soil liquefaction occurrences, such as sand boils and flows have been mapped in areas adjacent to Pinios and Titarissios rivers. The first area is located between the villages of Koutsochero to Pineiada and Zarko (Fig: 12), while the latter is less extended and is observed mainly in the area of Vlachogianni and Varko villages. The liquefaction phenomena were mapped in great detail using UAVs (Fig. 13). Comparison with current and historical satellite images, show that in the area of Pinios river the liquefaction is clearly associated with older abandoned meanders of the river, indicating a differentiated composition, more susceptible to liquefaction (Fig. 14). A liquefaction susceptibility map of Greece and an associated database (DALO v. 1.0) have been published by Papathanassiou and Pavlides, 2009 and Papathanassiou et al., 2010), whilst an evaluation of earthquake-induced liquefaction in the urban areas and more specific in Larissa city has been published by Papathanassiou et al. (2011).

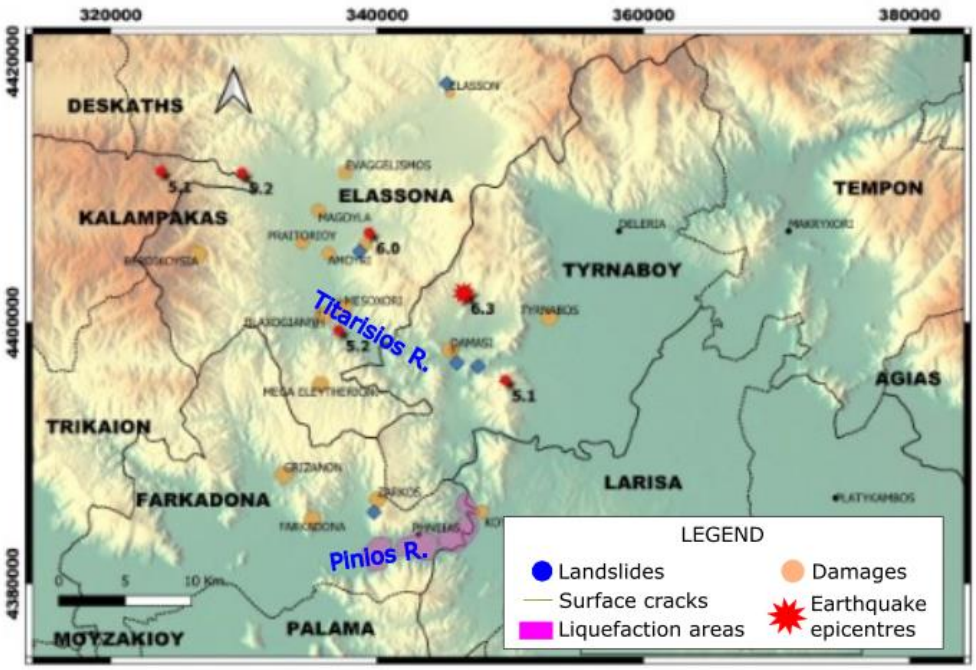

Fig. 10: Distribution map of the main surface effects that were observed in the meisoseismal area.

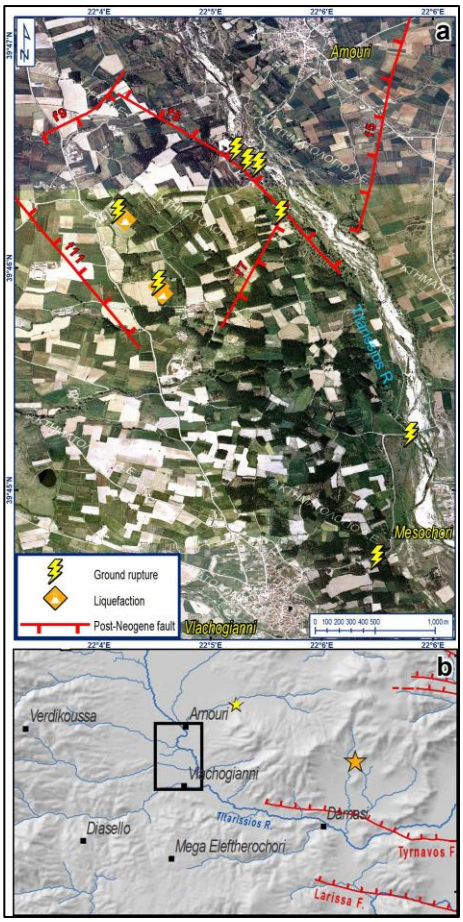

Fig. 11: Distribution of surface ruptures and liquefaction in Titarissios river valley, where the main bulk of the earthquake's surface effect was observed.

Fig: 12: Examples of sand flows, sand boils and lateral spreading in the liquefied area SE of Pineiada village.

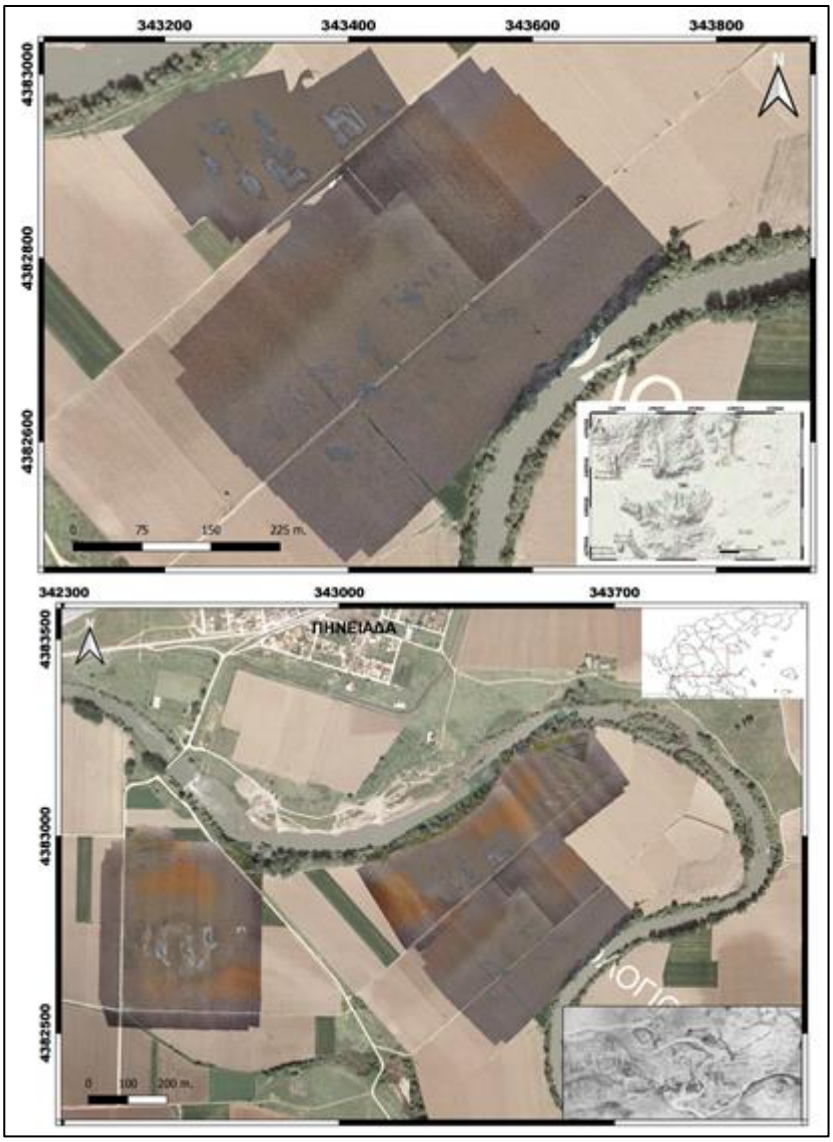

Fig. 13: Orthorectified image of the liquefied areas (gray spots). Images from a series of high-flying UAV campaigns have been combined with orthophotos from the Cadastral project of Greece.

Fig. 14: A detailed UAV composite orthophoto (yellow border) overprinted onto a satellite image, clearly shows that the distribution of individual liquefaction features (gray spots) coincides with an abandoned and filled bend of Pinios river. The current riverbed is visible at the right part of the map.

6.2. Rock falls, landslides and lateral spreading

Gravitational secondary effects, such as rock falls and landslides, were observed throughout the area (Fig. 15). Their distribution does not follow a specific pattern, but it is rather dependant of local site conditions, i.e., rock quality and slope angle. Lateral spreading was quite common in areas close to river banks, such as in Damasi, Mesochori, etc. (Fig. 16).

Fig. 15*:* Rock falls and slope failures along the country road to Vlachogianni village.

Fig. 16: Secondary cracks due to lateral spreading and associated liquefaction NW of Mesochori village.

7. GNSS DATA AND SITE DISPLACEMENT ESTIMATION

In order to estimate the influence of March 3, 2021 earthquake on site displacements a time period of fourteen days GNSS data was selected, from March 1 to March 14, 2021. Specifically, data for two days before and eleven days after the event were processed. The data extracted from five permanent GNSS stations located from 15 to 50 km away from the epicentre. GNSS stations are part of various networks such as HermesNet of Auth, HxGon SmartNet/Greece and NoaNet. Data analysis was based on 30-sec daily GPS+Glonass observations and elevation cut-off angle 10°. Four of the five stations record GPS and Glonass data which is an advance for the impact of Satellite geometry in the process. The process was held on the current reference frame ITRF2014 using the web-based PPP platform of National Resources of Canada- Canadian Geodetic Survey (CGS). The well-known CSRS-PPP is an online application for data post-processing allowing users to compute higher accuracy positions from their GNSS raw data. PPP technique uses zero-difference pseudoranges and carrier phase data utilizing precise orbits, clock values (retrieving from analysis centers) and models for account of satellite antenna offset and earth and ocean tide loading. This algorithm can potentially achieve high order positional accuracy. This is done in the present study because daily station data were processed. Also, the used platform has a modernization option which includes PPP with ambiguity resolution for data collected on or after 1 January 2018. Co-seismic displacements derived by daily processing scenarios, where the estimates of position coordinate characterized by sub-centimeter accuracy, is an appropriate level for our study. The maximum horizontal displacements were observed in ELAS (2.2 cm to the North and 4.3 cm to the East) and KLOK (3.4 cm to the South and 4 cm to the West) stations. These displacements are in accordance with the focal mechanism parameters, as well as with the long-term active extension direction, as discussed earlier. The daily calculated displacements expressed in the topocentric system (East, North, Up) are presented in the following table 1, while the timeseries of the horizontal displacements is shown in Fig 17.

Table 1. GNSS displacements.

GNSS station	Latitude	Longitude	dEast (m)	dNorth (m)	dUp (m)
ELAS	39.89243	22.20612	0.022	0.043	0.014
KLOK (GPS only)	39.56473	22.01438	-0.034	-0.040	0.003
KRDI	39.36348	21.92264	-0.003	-0.011	0.024
LARM	39.61410	22.38791	0.001	0.005	0.014
MURG	39.73871	21.55422	-0.004	-0.002	0.026

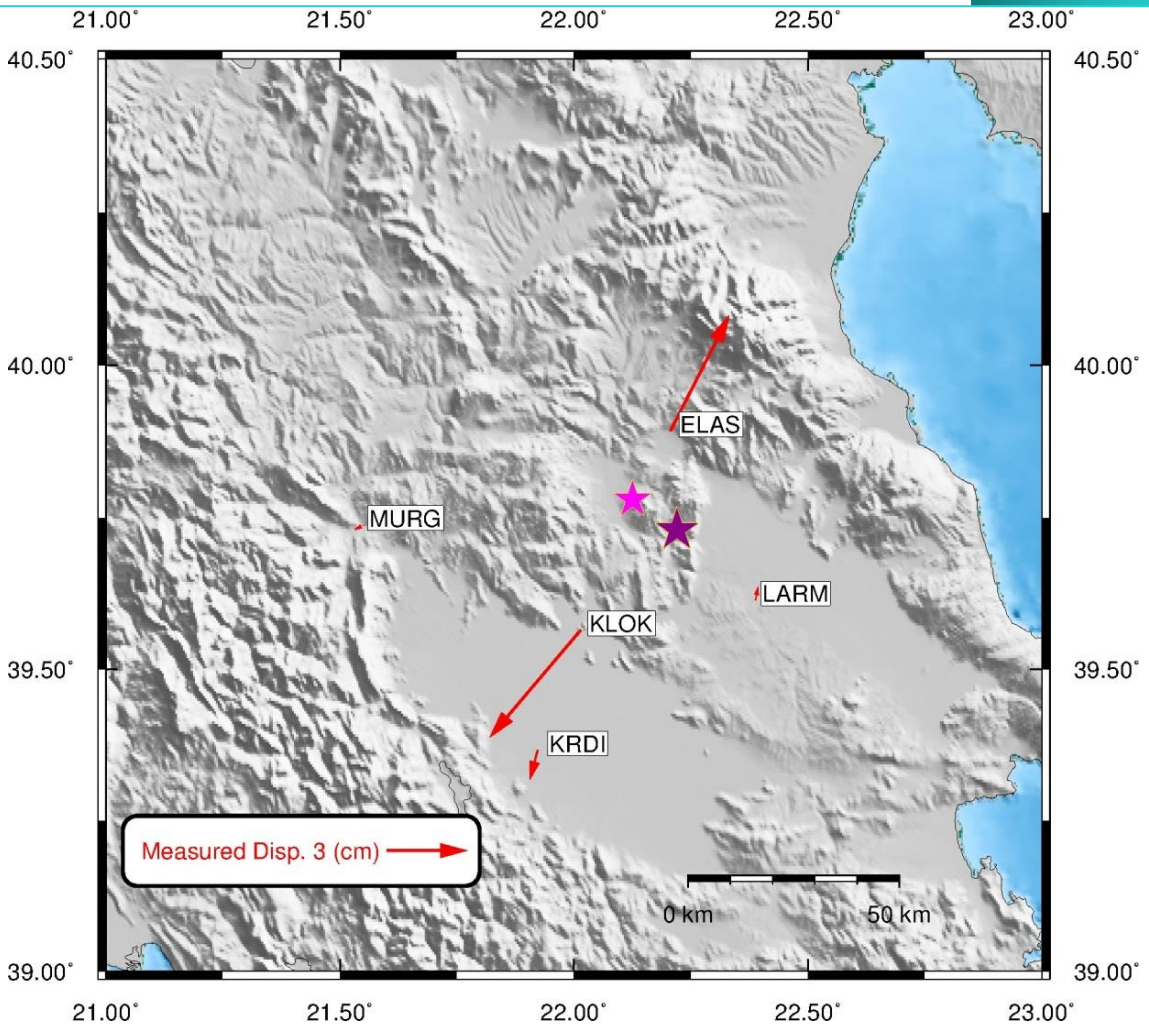

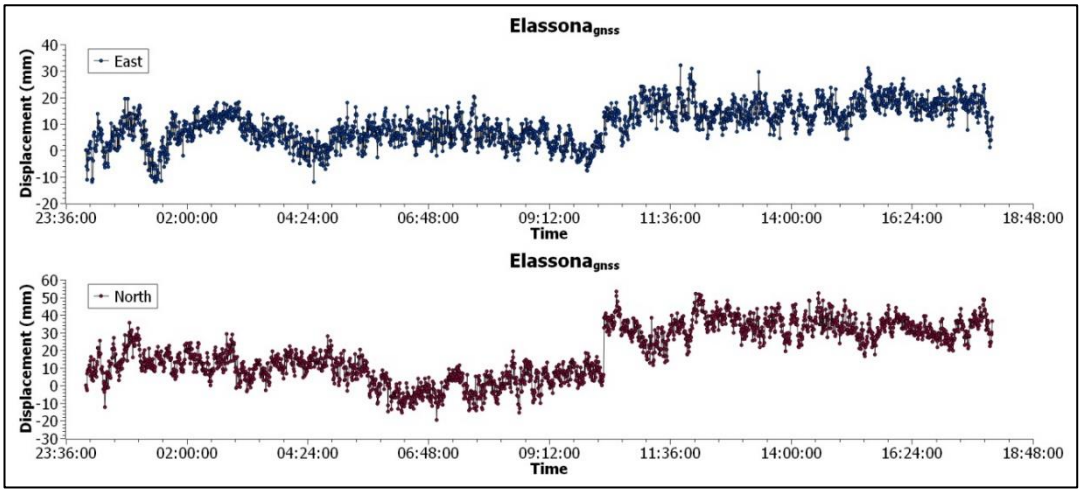

Fig. 17: Horizontal co-seismic displacements in the broader area of the earthquakes.

8. EARTH OBSERVATION MAPPING OF SECONDARY PHENOMENA

For the mapping of earthquake-induced secondary phenomena by means of Earth Observation (EO), Copernicus Sentinel-1 mission data covering the broader epicentral area were used. This comprise of Sentinel-1 imagery from four different tracks, namely two ascending (A102 & A175) and two descending (D007 & D080) satellite orbits. The imagery utilized, limited to scenes acquired immediately before and after of the mainshock, are shown in Table 2.

Table 2. Co-seismic Sentinel-1 interferometric pairs utilized in the current work.

Acquisition Geometry	Relative Orbit	Incidence Angle (degrees)	Acquisition Time (UTC)	Pre-event Acquisition Date	Post-event Acquisition Date	Temporal Separation (days)	Perpendicular Baseline (m)
Ascending	102	34	~16:25	25/02/2021	03/03/2021	6	-42.5
Ascending	175	44	~16:30	02/03/2021	08/03/2021	6	11.6
Descending	007	44	~04:30	03/03/2021	09/03/2021	6	47.6
Descending	080	34	~04:40	02/03/2021	08/03/2021	6	-54.2

Our approach is based on analysis and interpretation of co-seismic interferometric coherence products for the recognition of surface changes within the area of interest. Interferometric processing was undertaken on a Virtual Machine (VM) provided by the ESA RSS-Cloud Toolbox service (Marchetti et al., 2012), having direct access to the Copernicus archives via the CREODIAS infrastructure (https://creodias.eu). For the processing of the S-1 IW Single Look Complex (SLC) data, the GAMMA software packages were used (Papanikolaou et al., 2010; Foumelis et al., 2013; Wegnüller et al., 2016; Lemoine et al., 2020). To compensate for the topographic component, heights from the AW3D30 DSM (Takaku et al., 2018) were utilized. Although during the early response phase, and in order to rapidly aid in-situ observation, differential interferograms were generated using annotated orbits, for the current work we used precise orbit state vectors, with an accuracy better than 5 cm (Peter et al., 2017). The differential interferogram of the M6.3 mainshock, responsible for the majority of the secondary phenomena observed, is shown in Fig. 18.

For the estimation of coherence, the complex normalized interferogram and the two corresponding backscatter intensity images are used (Fig. 19). The applied estimator is adaptive, adjusting the window size to local coherence levels estimated in an initial non-adaptive step. Large estimation windows are applied for regions of low coherence,

reducing thus the bias, while small estimator windows in regions of high coherence maintain spatial resolution. To reduce temporal decorrelation effects, only interferometric pairs of 6-day time span were utilized (Table 2). The overall obtained high coherence levels allowed the identification of local low coherence patterns (Fig. 19), that could be attributed to earthquake-induced secondary effects (i.e., liquefaction and surface ruptures).

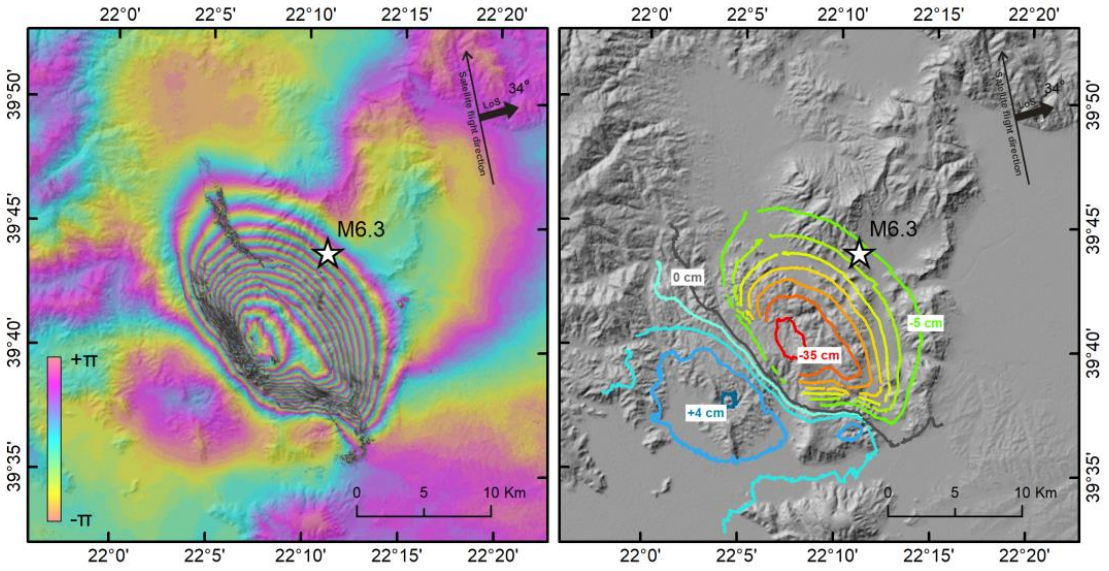

Fig. 18: Co-seismic differential interferogram of the M6.3 Tyrnavos earthquake using Sentinel-1 pre- (25/02/2021) and post-event (03/03/2021) scenes acquired along the ascending 102 orbit (left) and extracted displacement contours after phase unwrapping (right). The reference point is located outside the shown frame.

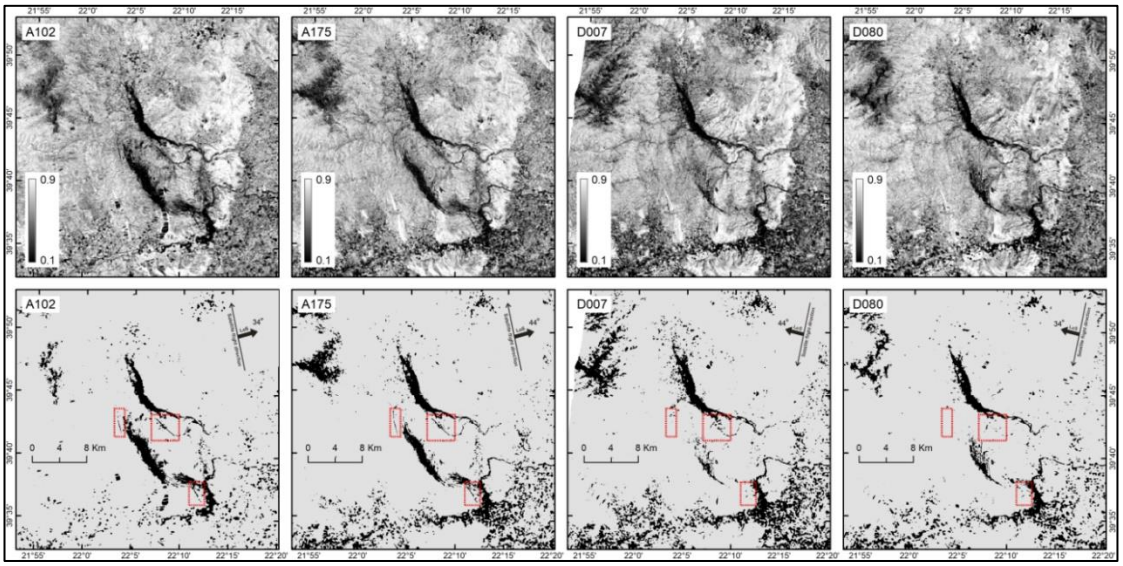

Fig. 19: Interferometric coherence of co-seismic pairs (see Table 1) acquired by different Sentinel-1 geometries (up) and extracted low coherence regions based on 0.3 thresholds (down). Note the narrow linear features in the red dotted polygons, visible only in ascending geometries due to favorable alignment between their trend and the LoS direction.

However, due to the influence of the SAR acquisition geometry as expressed by layover and shadow effects (mainly between ascending and descending orbits) as well as other short-term changes of the surface, several non-common regions of low coherence exist between the various coherence maps. Based on the assumption that secondary surficial effects caused by the earthquake should be present in all co-seismic interferometric pairs of comparable temporal coverage, only regions exhibiting low coherence values (below 0.3) in all considered pairs were accepted for further analysis. The above masking step reduced considerably the number of irrelevant (non-earthquake related) low coherence signals. Subsequent sieve filtering, as post-processing in a GIS environment, was still considered necessary to eliminate small low coherence cluster (2-3 pixels size), providing a much cleaner composite coherence output (Fig. 20).

Nevertheless, the above-mentioned procedure masked out actual linear low coherence features detectable only by single SAR geometry (see Fig. 19). This is more evident when the features, in principle narrow low coherence zones, are aligned more or less parallel to the Line-of-Sight (LoS) direction of the satellite. Developed mainly along the SW-NE direction, the north-westward looking descending orbit represents a non-favorable viewing condition. Thus, a complementary step involving visual interpretation of co-seismic differential interferograms was considered to outline discontinuities of the interferometric fringes (Fig. 21). That was proven equally valuable for the direct mapping of linear surface ruptures.

EO-detected surface ruptures seem constraint within the region affected by the M6.3 induced ground displacements, located south of the mainshock epicenter, maintaining a NW-SE trend (Fig. 21). The two major spatially continuous regions of low coherence collocate well with the Pinios and Titarissios River plains, can be attributed to extended liquefactions or other surface disturbance triggering phenomena. Finally, a decorrelated zones (coherence <0.3) of approximately 1.6 sq. km, located in the vicinity of the area where maximum ground displacements were observed (Fig. 21). This region can be associated to distributed deformation because of the propagation of motion caused by a blind seismic rupture to the surface.

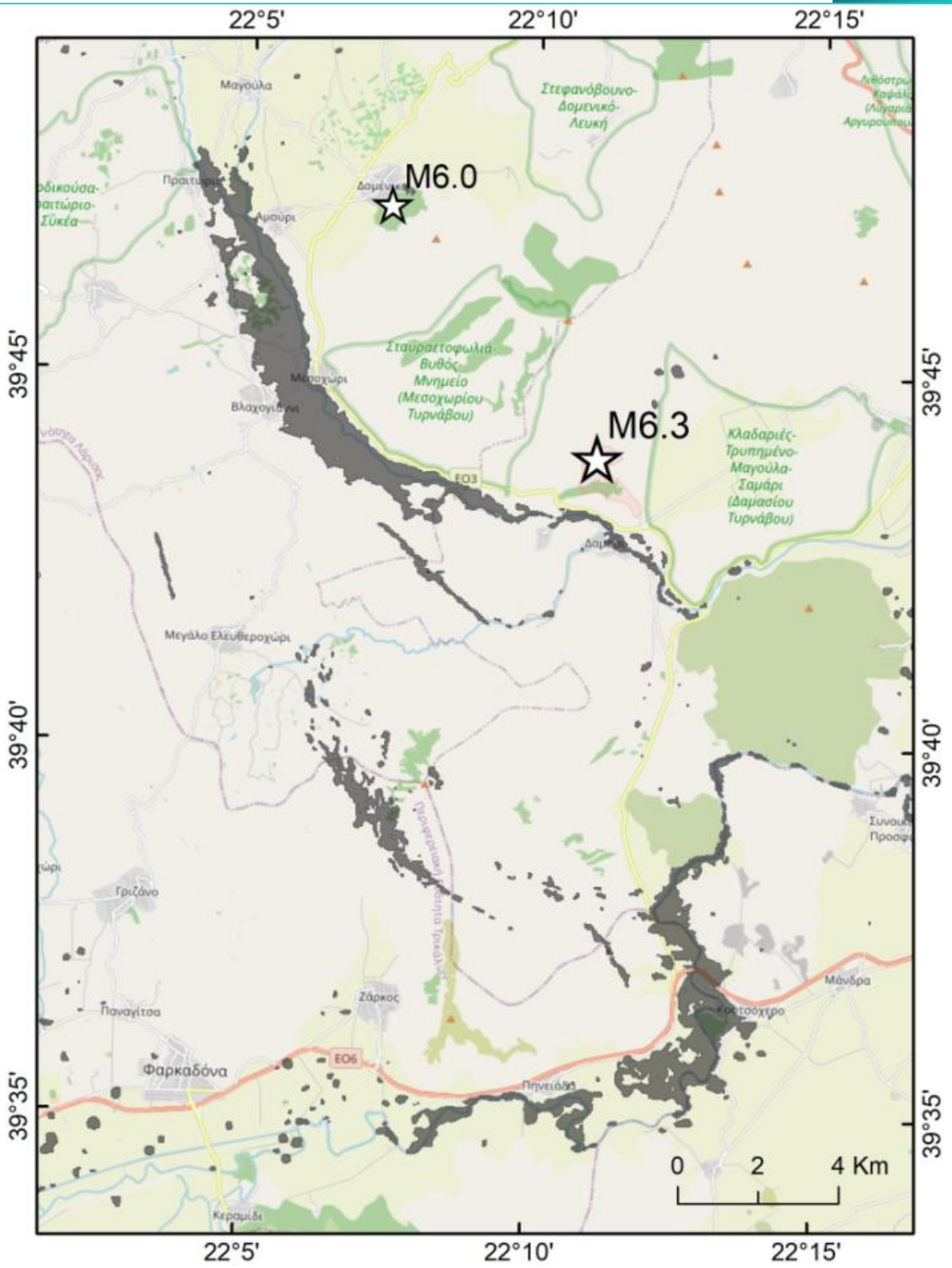

Fig. 20: Regions of low interferometric coherence (<0.3) as derived by combined analysis of independent coherence estimates from different acquisition geometries (see text for details). These low coherence regions, shown in grey, common to all examined co-seismic pairs (see Table 2), can be attributed to the secondary phenomena (i.e. liquefactions and surface ruptures) induced by the Tirnavos M6.3 mainshock.

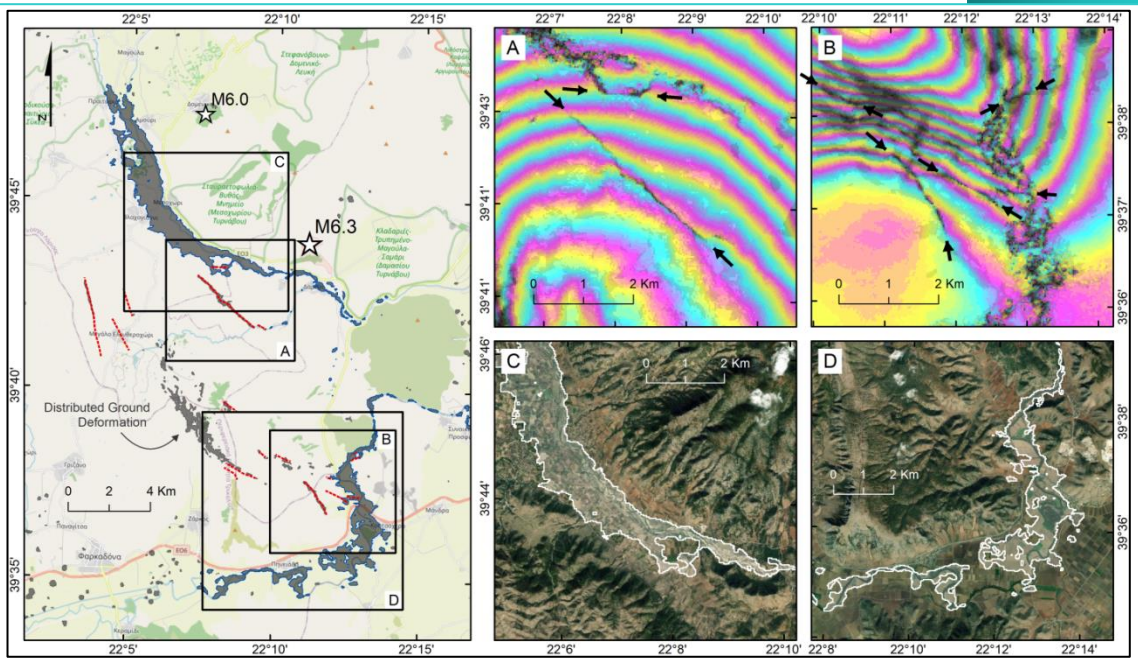

Fig. 21: Composite map of decorrelated areas (shaded polygons) as derived by analysis of co-seismic interferometric coherence estimates and surface ruptures (red dotted lines) by visual interpretation of fringes' spatial discontinuities (A and B). Regions suffered extended liquefactions (shaded polygons with blue outline) collocate with riverbeds (C and D).

9. THE NEW, PREVIOUSLY UNKNOWN, SEISMOGENIC FAUL

As far as the insofar unknown and unmapped seismic fault is concerned, fieldwork showed that there are characteristic geological indications in the Pelagonian continental basement rocks (e.g. Kilias and Mountrakis, 1987; Kilias et al., 1991), indicating that a moderate to low angle normal fault has acted as a hidden or blind fault during the earthquake. Field observations show that similar older normal faults in the basement close to the epicentre are dipping with angles ranging between 25° and 50°. Although the inferred dip angle of focal mechanisms 35-40° seems low, it is well within the range of seismogenic normal faults, as observed in global data sets (Jackson and White, 1989). It is associated with the bedrock schistosity, as well as with small high angle reverse faults of the Pelagonian anticline. The presumed seismic fault extends in the broader area between the villages of Zarko and Megalo Eleftherochori, as an inherited shear zone (Fig. 22). Geologic indications include outcrops of the post Alpine shear zone (Fig. 22a,b,c), located along the boundary between interferometrically-indicated uplift and subsidence terrains (Fig. 23, that is 0 line of displacement), the existence of cataclasite and fault gouge in the shear zone (Fig. 22a-e), which indicates reactivation of the fault in brittle conditions during the neotectonic period and slickenlines compatible with the active stress field (Fig. 22a,c,d). Fault surfaces strike at N160°E and dip at 50° on

average which is in good agreement to the published focal mechanisms by Greek (NOA and AUTh) and other international Institutes. Co-seismic indicators include small, ruptured fault surfaces with detached rock slabs and pieces, as well as small-scale soil fractures following the trace of the mapped fault (Fig. 22d,g), with negligible vertical displacement and small heave (up to 2 cm).

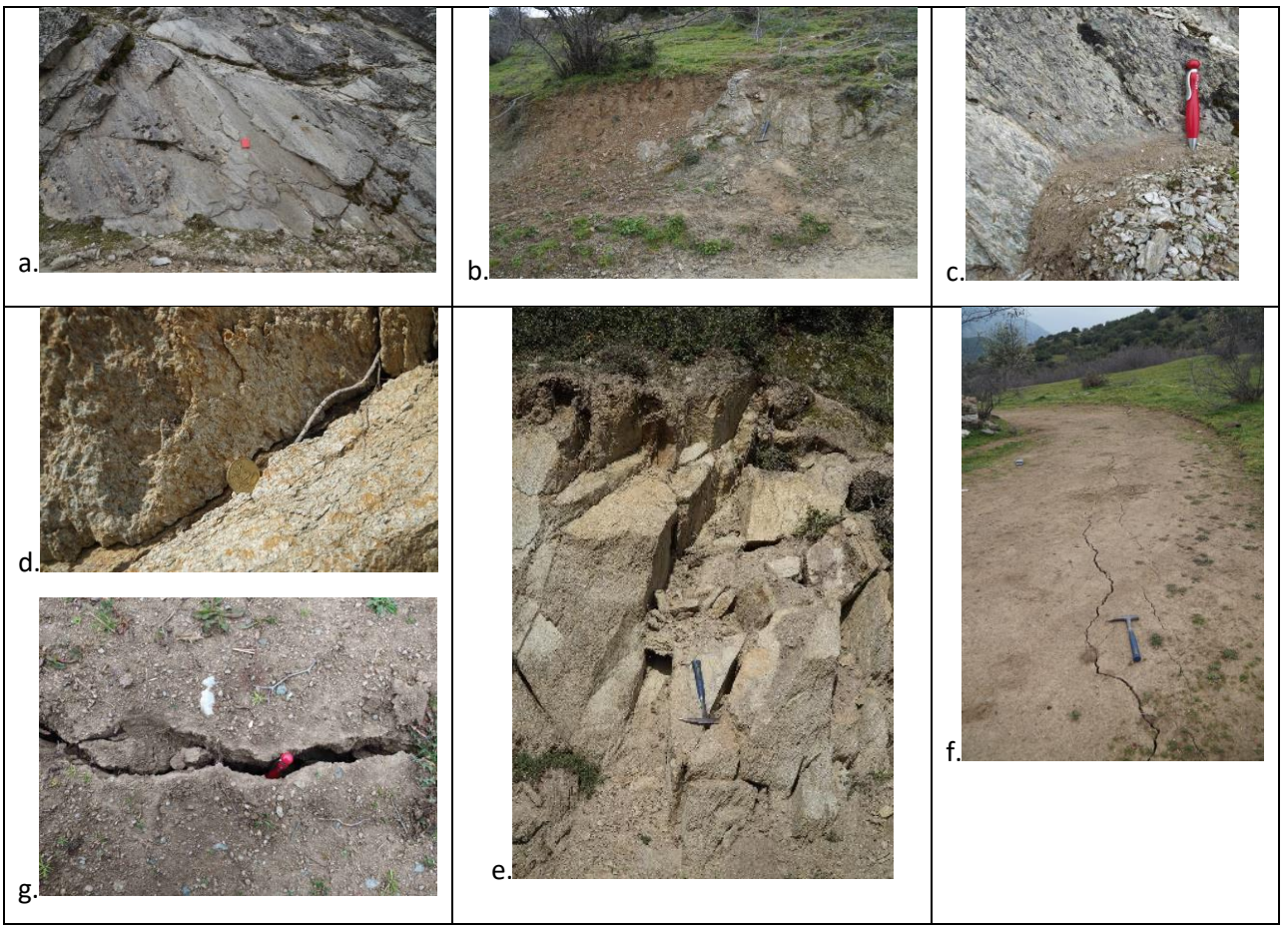

Fig. 22: a) Fault surface of the low-angle normal fault in the bedrock, believed to be a strand of the causative fault zone b) a zone of intense brittle shearing, accompanied by fault gouge and cataclasite within the low-angle normal fault zone c) fault surface d) opening along a pre-existing shear zone e) cataclasite and opening in Paleozoic crystalline rocks f & g) co-seismic surface cracks in the soil cover, following the inferred strike and location of the causative fault zone in the bedrock.

The seismic fault model (seismic source) of the mainshock is based on the GFZ's moment tensor solution (strike: 130°, dip: 45°, rake: -90°), the scalar relationships of Wells & Coppersmith (1994; length and width), and the interferograms along with the site observations (position). We calculated the Coulomb static stress changes for receiver faults similar to the seismic source at a depth of 8 km. A vertical cross-section normal to the source's strike is also calculated. Results show stress-load beyond the tips of the fault, suggesting a triggering scenario for faults of similar geometry and kinematics located in this red area (Fig. 23). The northwestern edge of the fault (red-

yellow) was activated during the second event of 4th of March. The seismic source is also used to model the vertical displacement on the ground after using the Okada formulae (Fig. 23). The maximum calculated vertical displacement is 2.93 cm. Both Coulomb and Okada calculations were performed with the Coulomb v. 3.3 application (Lin and Stein, 2004; Toda et al., 2011).

a.

b.

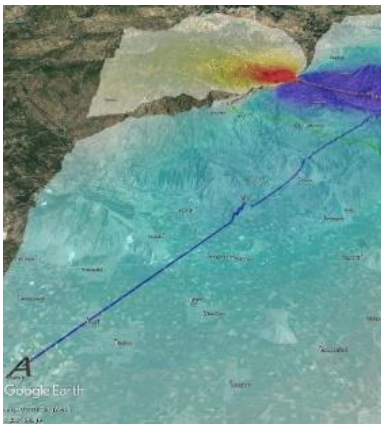

c.

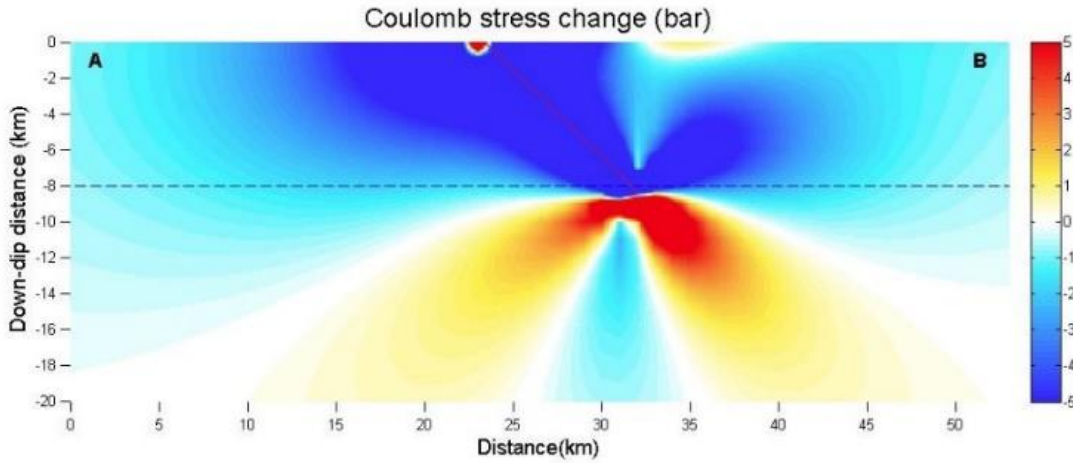

Fig. 23: a) A preliminary model of the seismic source is showing vertical displacement on the ground b) The seismic fault model (seismic source) of the mainshock is based on the GFZ's moment tensor solution. The Coulomb static stress changes (seismic source at a depth of 8 km). (c) Vertical cross-section normal to the source's strike (A-B). Results show stress-load beyond the tips of the fault, suggesting a triggering scenario for faults of similar geometry and kinematics located in this red area.

10. CONCLUDING REMARKS

The fault that ruptured in 2021 cannot be associated with any of the previously known active faults in the area. Field work, seismological data and InSAR results show that the main seismogenic structure is neither the well-studied active fault of Tyrnavos, nor

the extension to the NW of the also well-known fault of Larissa, although both appear to have been activated and partially affected by the main seismic fault as secondary triggered structures. A NE-dipping normal fault was activated for the main event as a blind or buried fault, following pre-existing inherited alpine structures, that does not appear to have a surficial expression. The strongest aftershock or second main earthquake of 4th of March (M_w 6.0) is within the same rupture area, but may have been produced by a secondary adjacent segment of the same fault zone in the seismic sequence site. Based on the overall results of the work performed in this paper, we propose the model of Fig. 24. The main seismogenic structure is a low-angle normal detachment fault that dips towards the NE, while the steeper dipping mapped active faults that reach the surface are interpreted as supra-detachment structures. They occasionally have been activated as triggered faults, as indicated by minor co-seismic surface ruptures along the Titarissios valley fault, the Zarkos shear zone and the presumed extension of Tyrnavos fault to the WNW. This fault configuration is compatible with the post-orogenic collapse pattern, which caused crustal thinning and exhumation of lower tectonostratigraphic units throughout the broader area.

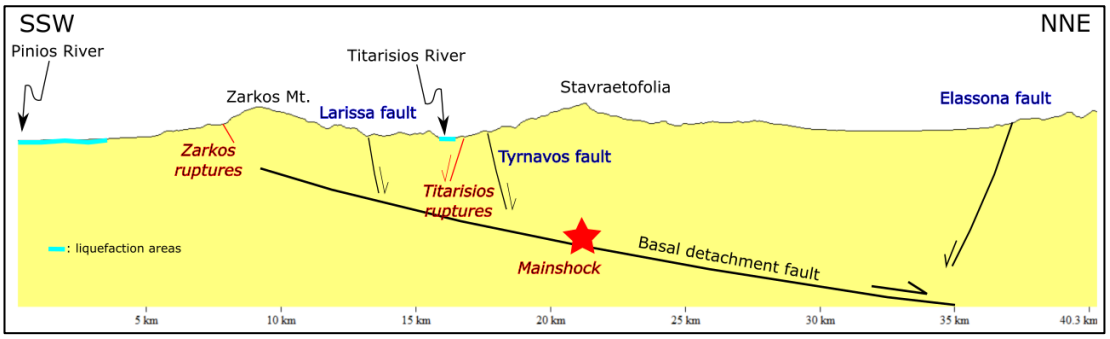

Fig. 24: Interpretive sketch of the assumed tectonic structure of the area, based on geological and seismological data.

The active stress pattern of the Thessalian upper crust in the area is characterized by extension in an NNE-SSW direction. This is based in both Quaternary neotectonic quantitative methods and focal mechanisms of recent earthquakes (Fig. 8). The older Neogene-Pliocene extensional field had a different tensile direction (NE-SW, Pavlides and Mountrakis, 1987; Mercier et al., 1989; Caputo and Pavlides, 1993). The Neogene-Quaternary Elassona-Potamia basin shows that in addition to the ESE-WNW trending faults (~110°) that are favourably oriented to the active tectonic field, inherited NW-SE directed faults can also be activated. The analysis of the focal mechanisms of the latest earthquakes seems to be related to the active field of trends and faults that tend to create new structures in the area, proving its continuous and gradual geological evolution. At

the same time, however, this earthquake raises new substantive questions and concerns, while revising some established views, such as:

(a) The status of active stress trends.
(b) The direction of active tectonic structures.
(c) The existence of a seismogenic fault in a mountainous volume of crystalline rocks without typical geomorphological expression.
(d) The role of blind faults to Seismic Hazard Assessment.

11. ACKNOWLEDGEMENTS

The authors are grateful to Assoc. Prof. Sotirios Kokkalas and Dr. Christoph Gruetzner, whose valuable comments have greatly improved the manuscript. We would also like to thank the Editor-in-Chief Dr. Athanasios Ganas for his assistance in the final format of the manuscript.

12. REFERENCES

Ambraseys, N., 2009. Earthquakes in the Mediterranean and Middle East. Cambridge University Press, Cambridge. https://doi.org/10.1017/CBO9781139195430

Caputo, R., 1995. Inference of a seismic gap from geological data: Thessaly (Central Greece) as a case study. *Annals of Geophysics*, *38*. https://doi.org/10.4401/ag-4127

Caputo, R., Chatzipetros, A., Pavlides, S., Sboras, S., 2013. The Greek Database of Seismogenic Sources (GreDaSS): state-of-the-art for northern Greece., *Annals of Geophysics*. https://doi.org/10.4401/ag-5168

Caputo, R., Chatzipetros, A., Pavlides, S., Sboras, S., 2012. The Greek Database of Seismogenic Sources (GreDaSS): state-of-the-art for northern Greece. *Annals of Geophysics*, 55, 859–894. https://doi.org/10.4401/ag-5168

Caputo, R., Helly, B., Pavlides, S., Papadopoulos, G., 2004. Palaeoseismological investigation of the Tyrnavos Fault (Thessaly, Central Greece). *Tectonophysics*, 394, 1–20. https://doi.org/10.1016/j.tecto.2004.07.047

Caputo, R., Pavlides, S., 2013. Greek Database of Seismogenic Sources (GreDaSS)., University of Ferrara, Italy. https://doi.org/10.15160/UNIFE/GREDASS/0200

Caputo, R., Pavlides, S., 1993. Late Cainozoic geodynamic evolution of Thessaly and surroundings (central-northern Greece). *Tectonophysics*, 223, 339–362. https://doi.org/10.1016/0040-1951(93)90144-9

Caputo, R., Pavlides, S., GreDaSS Working Group, 2014. The Greek Database of Seismogenic Sources (GreDaSS): the new version. *EGU General Assembly 2014*.

Chatzipetros, A., Lazos, I., Pavlides, S., Pikridas, C., Bitharis, S., 2018. Determination of the active tectonic regime of Thessaly, Greece: a geodetic data based approach. *XXI International Congress of the CBGA*. Salzburg, 227.

Dinter, D.A., Royden, L., 1993. Late Cenozoic extension in northeastern Greece: Strymon Valley detachment system and Rhodope metamorphic core complex. *Geology*, 21, 45–48. https://doi.org/10.1130/0091-7613(1993)021

Forster, M.A., Lister, G.S., 1999. Detachment faults in the Aegean core complex of Ios, Cyclades, Greece. *Geological Society, London, Special Publications*, 154, 305–323. https://doi.org/10.1144/GSL.SP.1999.154.01.14

Foumelis, M., Trasatti, E., Papageorgiou, E., Stramondo, S., Parcharidis, I., 2013. Monitoring Santorini volcano (Greece) breathing from space. *Geophysical Journal International*, 193, 161–170. https://doi.org/10.1093/GJI/GGS135

Galanakis, D., Sboras, S., Konstantopoulou, G., & Xenakis, M. 2021. Neogene-Quaternary tectonic regime and macroseismic observations in the Tyrnavos-Elassona broader epicentral area of the March 2021, intense earthquake sequence. Bulletin of the Geological Society of Greece, 58, 200-221. doi:https://doi.org/10.12681/bgsg.27196

Ganas, A., Valkaniotis, S., Tsironi, V., Karasante, I., Elias, P., Kapetanidis, V., Kasssaras, I., Papathanassiou, G., Briole, P., 2021. The March 2021 seismic sequence in Larisa - Damasi , Thessaly (central Greece), its seismotectonic characteristics and geodynamic effects. https://doi.org/10.5281/ZENODO.4617264

Jackson, J.A., White, N.J., 1989. Normal faulting in the upper continental crust: observations from regions of active extension. *Journal of Structural Geology*, 11, 15–36. https://doi.org/10.1016/0191-8141(89)90033-3

Kilias, A., 1995. Tectonic evolution of the Olympus - Ossa mountains : emplacement of the blueschists unit in eastern Thessaly and exhumation of Olympus - Ossa carbonate dome as a resault of tertiary extension (Central Greece). *Mineral Wealth*, 96, 7–22.

Kilias, A., Alonso-Chaves, F.M., Orozco, M., Tranos, M., Soto, J., 2002. Extensional collapse of the Hellenides: a review. . *Rev. Soc. Geol. España,* 15, 129–139.

Kilias, A., Falalakis, G., Sfeikos, A., Papadimitriou, E., Vamvaka, A., Gkarlaouni, C., 2013a. The Thrace basin in the Rhodope province of NE Greece - A Tertiary supradetachment basin and its geodynamic implications. *Tectonophysics*, 595–596, 90–105. https://doi.org/10.1016/j.tecto.2012.05.008

Kilias, A., Fasoulas, C., Priniotakis, M., Sfeikos, A., Frisch, W., 1991. Deformation and HP/LT Metamorphic Conditions at the Tectonic Window of Kranea (W -- Thessaly, Northern Greece). *Zeitschrift Der Deutschen Geologischen Gesellschaft*, 142, 87–96. https://doi.org/10.1127/zdgg/142/1991/87

Kilias, A., Mountrakis, D., 1989. The Pelagonian nappe: tectonics, metamorphism and magmatism. *Bulletin of the Geological Society of Greece*, 23, 29–46.

Kilias, A., Mountrakis, D., 1987. Structural Geology of the Central Pelagonian Zone (Kamvounia Mountains, North Greece). *Zeitschrift Der Deutschen Geologischen Gesellschaft*, 138, 211–237. https://doi.org/10.1127/zdgg/138/1987/211

Kilias, A., Thomaidou, E., Katrivanos, E., Vamvaka, A., Fassoulas, C., Pipera, K., Falalakis, G., Avgerinas, S., Sfeikos, A., 2016. A geological cross-section through Northern Greece from Pindos to Rhodope mountain ranges: A field guide across the external and internal hellenides. *Journal of the Virtual Explorer*, 50, 1–107. https://doi.org/10.3809/jvirtex.2016.08685

Kilias, A., Vamvaka, A., Falalakis, G., Sfeikos, A., Papadimitriou, E., Gkarlaouni, C., Karakostas, B., 2013b. The Mesohellenic trough and the Thrace Basin. Two Tertiary molassic Basins in Hellenides: do they really correlate? *Bulletin of the Geological Society of Greece*, 47, 551. https://doi.org/10.12681/bgsg.11082

Koroneos, A., Kilias, A., Avgerinas, A., 2013. Hercynian plutonic rocks of Voras Mountain, Macedonia, Northern Greece: Their structure, petrogenesis, and tectonic significance. *International Geology Review*, 55, 994–1016. https://doi.org/10.1080/00206814.2012.758830

Kremastas, E., Pavlides, S., Chatzipetros, A., Koukouvelas, I., Valkaniotis, S., 2018. Mapping the Gyrtoni Fault (Thessaly, Central Greece) using an Unmanned Aerial Vehicle. 9th International INQUA Meeting on Paleoseismology, *Active Tectonics and Archeoseismology (PATA)*, 126–129.

Lazos, I., Pikridas, C., Chatzipetros, A., Pavlides, S., 2021. Determination of local active tectonics regime in central and northern Greece, using primary geodetic data. *Applied Geomatics*, 13, 3–17. https://doi.org/10.1007/s12518-020-00310-x

Lemoine, A., Briole, P., Bertil, D., Roullé, A., Foumelis, M., Thinon, I., Raucoules, D., de Michele, M., Valty, P., Colomer, R.H., 2020. The 2018-2019 seismo-volcanic crisis east of Mayotte, Comoros islands: Seismicity and ground deformation markers of an exceptional submarine eruption. *Geophysical Journal International*, 223, 22–44. https://doi.org/10.1093/GJI/GGAA273

Lin, J., Stein, R.S., 2004. Stress triggering in thrust and subduction earthquakes and stress interaction between the southern San Andreas and nearby thrust and strike-slip faults. *Journal of Geophysical Research: Solid Earth*, 109, 2303. https://doi.org/10.1029/2003JB002607

Lister, G.S., Banga, G., Feenstra, A., 1984. Metamorphic core complexes of Cordilleran type in the Cyclades, Aegean Sea, Greece. *Geology*, 12, 221–225. https://doi.org/10.1130/0091-7613(1984)12<221:MCCOCT>2.0.CO;2

Marchetti, P.G., Bivolta, G., D'Elia, S., Farres, J., Mason, G., Gobron, N., 2012. A Model for the Scientific Exploitation of Earth Observation Missions: The ESA Research and Service Support. *IEEE Geoscience and Remote Sensing*, 10–18.

Mercier, J.L., Sorel, D., Vergely, P., Simeakis, K., 1989. Extensional tectonic regimes in the Aegean basins during the Cenozoic. *Basin Research*, 2, 49–71. https://doi.org/10.1111/j.1365-2117.1989.tb00026.x

Mountrakis, D.M., 2006. Tertiary and Quaternary tectonics of Greece, *Geological Society of America Special Papers*. Geological Society of America. https://doi.org/10.1130/0-8137-2409-0

Papaioannou, I., 2019. The Larisa, Tyrnavos and Agia earthquake of 1892 [in Greek].

Papaioannou, I., 2018. The Larisa earthquake of March 1, 1941 [in Greek].

Papaioannou, I., 2017a. Earthquake activity in Thessaly during 16th-18th centuries [in Greek]., *Thessaliko Imerologio*, 353–396.

Papaioannou, I., 2017b. Earthquake activity in Thessaly during the 19th century [in Greek]., *Thessaliko Imerologio*, 273–292.

Papanikolaou, I.D., Foumelis, M., Parcharidis, I., Lekkas, E.L., Fountoulis, I.G., 2010. Deformation pattern of the 6 and 7 April 2009, MW=6.3 and MW=5.6 earthquakes in L'Aquila (Central Italy) revealed by ground and space based observations. *Natural Hazards and Earth System Science*, 10, 73–87. https://doi.org/10.5194/NHESS-10-73-2010

Papathanassiou, G.., Seggis, K.., Pavlides, S.., 2011. Evaluating earthquake-induced liquefaction in the urban area of Larissa, Greece. *Bulletin of Engineering Geology and the Environment*, 70, 79–88. https://doi.org/10.1007/s10064-010-0281-3

Papathanassiou, G., Pavlides, S., 2009. GIS-based DAtabase of historical Liquefaction Occurrences in broader Aegean region, DALO v1.0. *Proceedings of the XVII International Conference on Soil Mechanics &Amp; Geotechnical Engineering, Earthquake Geotechnical Engineering Satellite Conference*. https://doi.org/refwid:13962

Papathanassiou, G., Valkaniotis, S., Chaztipetros, A., Pavlides, S., 2010. Liquefaction susceptibility map of Greece. *Bulletin of the Geological Society of Greece*, 43, 1383. https://doi.org/10.12681/bgsg.11314

Papazachos, B.C., Papazachou, C.B., 2003. The earthquakes of Greece [in Greek], Second edi. ed. Ziti Editions, Thessaloniki.

Pavlides, S., Caputo, R., 2004. Magnitude versus faults' surface parameters: quantitative relationships from the Aegean Region. *Tectonophysics*, 380, 159–188. https://doi.org/10.1016/j.tecto.2003.09.019

Pavlides, S., Chatzipetros, A., Sboras, S., Kremastas, E., Chatziioannou, A., 2021. The northern Thessaly strong earthquakes of March 3 and 4 and their neotectonic setting. https://doi.org/10.5281/ZENODO.4618188

Pavlides, S., Kilias, A., 1987. Neotectonic and active faults along the Serbomacedonian zone (SE Chalkidiki, northern Greece). *Annales Tectonicae*, 1, 97–104.

Pavlides, S.B.B., Mountrakis, D.M.M., 1987. Extensional tectonics of northwestern Macedonia, Greece, since the late Miocene. *Journal of Structural Geology*, 9, 385–392. https://doi.org/10.1016/0191-8141(87)90115-5

Peter, H., Jäggi, A., Fernández, J., Escobar, D., Ayuga, F., Arnold, D., Wermuth, M., Hackel, S., Otten, M., Simons, W., Visser, P., Hugentobler, U., Féménias, P., 2017. Sentinel-1A – First precise orbit determination results. *Advances in Space Research*, 60, 879–892. https://doi.org/10.1016/J.ASR.2017.05.034

Sboras, S., 2011. The Greek Database of Seismogenic Sources: seismotectonic implications for North Greece. Pubblicazioni Dello IUSS 5, 1–274.

Sboras, S., Pavlides, S., Caputo, R., Chatzipetros, A., Michailidou, A., Valkaniotis, S., Papathanassiou, G., 2014. The use of geological data to improve SHA estimates in Greece. *Bollettino Di Geofisica Teorica Ed Applicata*, 55. https://doi.org/10.4430/bgta0101

Sfeikos, A., Böhringer, C., Frisch, W., Kilias, A., Ratschbacher, L., 1991. Kinematics of the Pelagonian nappes in the Kranea area, N. Thessaly (Greece). *Bulletin of the Geological Society Greece*, 25, 101–115. https://doi.org/refwid:11747

Takaku, J., Tadono, T., Tsutsui, K., Ichikawa, M., 2018. Quality improvements of "AW3D" global DSM derived from ALOS PRISM. *International Geoscience and Remote Sensing Symposium (IGARSS) 2018-July*, 1612–1615. https://doi.org/10.1109/IGARSS.2018.8518360

Toda, S., Stein, R.S., Sevilgen, V., Lin, J., 2011. Coulomb 3.3 Graphic-rich deformation and stress-change software for earthquake, tectonic, and volcano research and teaching-user guide, Open-File Report. https://doi.org/10.3133/OFR20111060

Tsodoulos, I., Stamoulis, K., Caputo, R., Koukouvelas, I., Chatzipetros, A., Pavlides, S., Gallousi, C., Papachristodoulou, C., Ioannides, K., 2016. Middle–Late Holocene earthquake history of the Gyrtoni Fault, Central Greece: Insight from optically stimulated luminescence (OSL) dating and paleoseismology. *Tectonophysics*, 687. https://doi.org/10.1016/j.tecto.2016.08.015

Valkaniotis, S., Papathanassiou, G., Ganas, A., Kremastas, E., Caputo, R., 2021. Preliminary report of liquefaction phenomena triggered by the March 2021 earthquakes in Central Thessaly, Greece. https://doi.org/10.5281/ZENODO.4608365

Wegnüller, U., Werner, C., Strozzi, T., Wiesmann, A., Frey, O., Santoro, M., 2016. Sentinel-1 Support in the GAMMA Software. *Procedia Computer Science*, 100, 1305–1312. https://doi.org/10.1016/J.PROCS.2016.09.246

Wells, D.L., Coppersmith, K.J., 1994. New empirical relationships among magnitude, rupture length, rupture width, rupture area, and surface displacement. *Bulletin of the Seismological Society of America*, 84, 974–1002.